Studies on anti-influenza virus action and active ingredients of *Citrullus lanatus* var. *citroides*

カラハリスイカ果汁の抗インフルエンザウイルス作用と有効成分に関する研究

2023

Ryosuke Morimoto

Doctoral Thesis at Mukogawa Women's University

Index

List of Abbreviations

AhR	:	Allyl hydrogen receptor
BSA	:	Bovine serum albumin
CDC	:	Center for disease control and prevention
cDNA	:	Complementary DNA
DAPI	:	4',6-diamidino-2-phenylindole
DMEM	:	Dulbecco's modified eagle's medium
EC	:	Epicatechin
EGC	:	Epigallocatechin
EGCG	:	Epigallocatechin gallate
E-MEM	:	Eagle's minimum essential medium
ESI	:	Electro spray ionization
FBS	:	Fetal bovine serum
FFRA	:	Focus-forming reduction assay
FFU	:	Focus-forming unit
HA	:	Hemagglutinin
HEK293	:	Human embryonic kidney cells 293
HI	:	Hemagglutination inhibition
ICTV	:	International committee on taxonomy of viruses
IgG	:	Immunoglobulin G
M	:	Matrix
MDCK	:	Madin-darby canine kidney
MOI	:	Multiplicity of infection
mRNA	:	messenger RNA
MS	:	Mass spectrometry
NA	:	Neuraminidase
NMR	:	Nuclear magnetic resonance
NP	:	Nucleoprotein
Nrf2	:	Nuclear factor E2-related factor 2
RNP	:	Ribonucleoprotein complex
PBS	:	Phosphate-buffered saline

PN	:	Prenylated naringenin
PR8/34	:	Puerto Rico/8/34
SARS-CoV-2	:	SARS-corona virus-2, COVID-19
SI	:	Selectivity index
WHO	:	World health organization
WM	:	Watermelon
WMJ	:	Watermelon juice
WWM	:	Wild watermelon (*Citrullus lanatus* var. *citroides*)
WWMJ	:	Wild watermelon juice

General Introduction

Humans and microorganisms have coexisted since ancient times, and many bacteria and viruses have been identified today. Yersinia pestis, vibrio cholera, variola virus, influenza virus and the coronavirus have caused many pandemics around the world [1]. In contrast to bacteria that can self-replicate with adequate nutrition and water, viruses are minute structures composed of protein shells and nucleic acids, infect host cells and are capable of self-replication.

Influenza virus is classified as envelope virus, single-stranded negative-strand RNA, and belong to the family *Orthomyxoviridae* [2]. The structure of influenza virus is composed of various proteins and genes (Figure 1), it is classified into types A, B, and C depending on the antigenicity of the M protein and NP. However, type D, which infects cattle and pigs, has been newly reported [3]. Furthermore, type A is classified into multiple subtypes and strains according to the antigenic differences in the spike glycoproteins, HA and NA, and 18 types of HA and 11 types of NA have been reported. There are subtypes from H1N1 to H18N11 (Figure 2). Also, Type B is roughly divided into B/Victoria/2/87 and B/Yamagata/16/88 based on the antigenicity of HA [4].
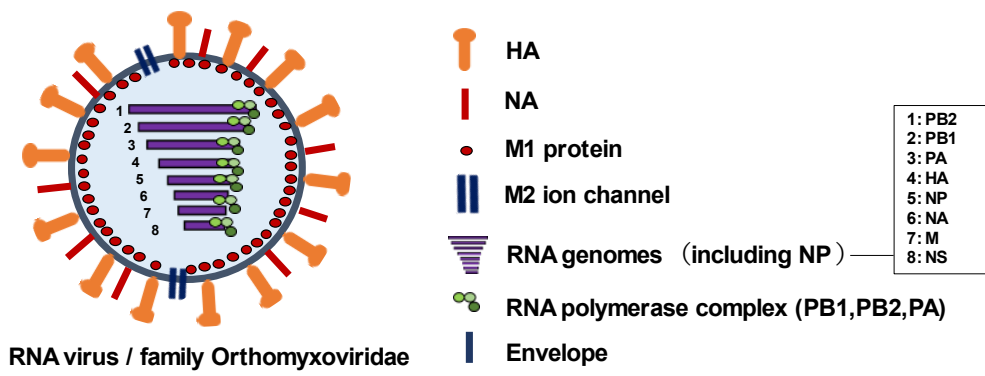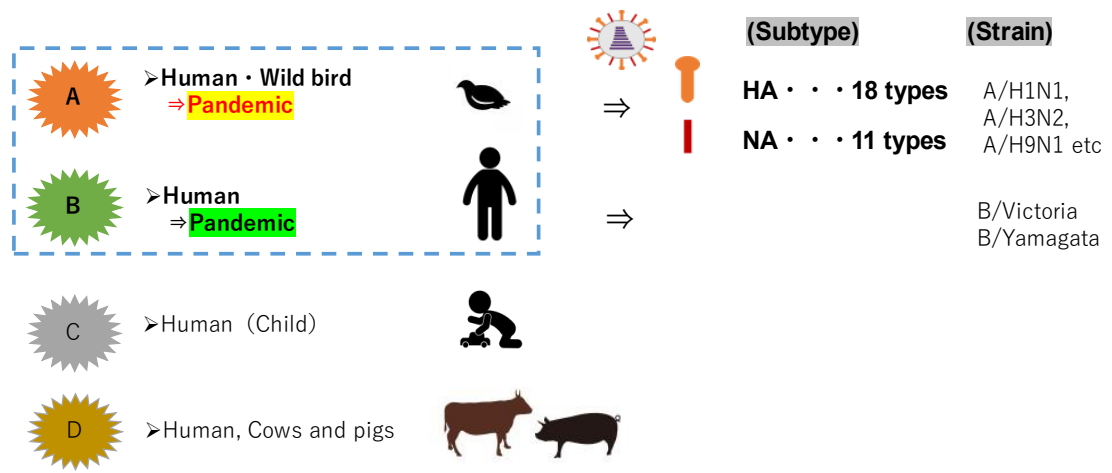
Figure 1. Structure of influenza virus

Figure 2. Types of influenza viruses and infected mammals

After infection, symptoms such as fever, headache, general malaise, muscle pain, arthralgia, cough, and nasal discharge continue, and begin to improve. However, it is known that the elderly, children, and patients with lifestyle-related diseases are at increased risk of complications and death [5-7].

Figure 3 shows the intracellular growth process of influenza A virus. Influenza viruses

recognize glycoproteins on the host cell membrane (**Step 1**). Virus particles are passively taken up into the cell by endocytosis, the host cell's foreign body uptake mechanism (**Step 2**). Virus particles are cleaved of HA by acidification in intracellular endosomes (**Step 3**), membrane fusion is followed by uncoating (**Step 4**). HA, one of the viral spike proteins, plays an important role in these processes [8]. The viral genome released into the cytoplasm moves into the nucleus in the form of RNP (**Step 5**), where virus-derived genomes are transcribed and replicated (**Step 6**). Virus-derived mature mRNA binds to the ribosome of the host cell, and NP, RNA polymerase (PA, PB1, PB2) and HA, NA, M protein are synthesized (**Step 7**). The synthesized RNA polymerase and NP are transported into the host nucleus, form vRNPs, and the vRNPs are transported into the cytoplasm (**step 8**), they reassemble with membrane proteins and others to form viral particles (**step 9**). Finally, new progeny viruses are released outside the cell (**Step 10**). In this process, NA plays an important role in separating sugar chains on the cell surface. To date, anti-influenza drugs have been developed that target each replication process of the virus (**Steps 4**, **6**, and **10**) as one of the strategies against influenza virus.
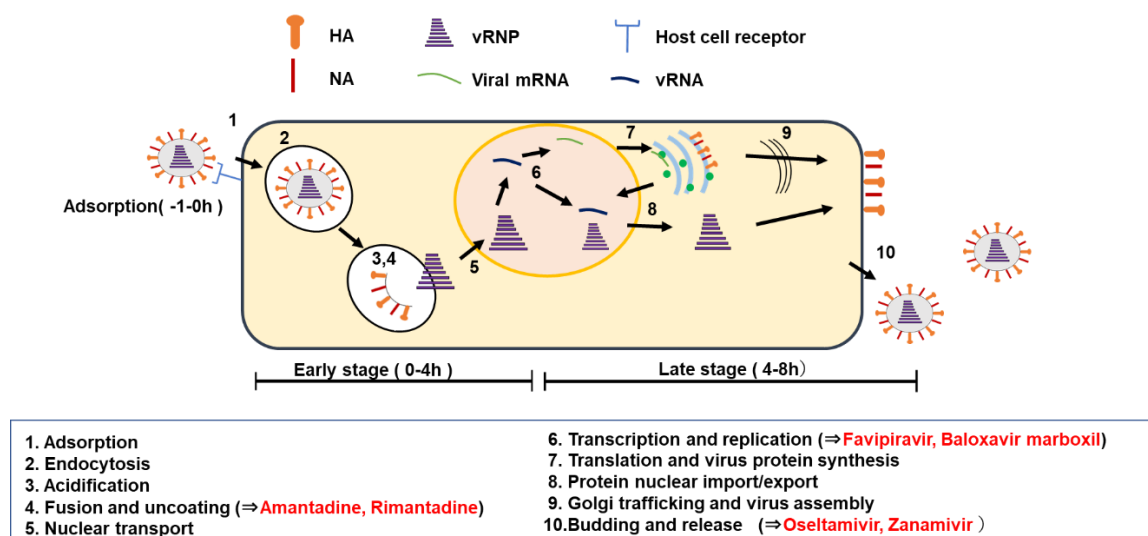
Figure 3. Viral growth steps and antiviral drugs

Viruses belonging to RNA viruses (SARS-CoV-2, Influenza virus) cause long-term epidemics due to antigenic mutations (continuous and discontinuous mutations) in viral proteins [9, 10], often leads to changes in viral immune susceptibility, drug susceptibility, cell tropism, and host range, and causes a decrease in preventive and therapeutic efficacy and emerging and re-emerging infectious diseases.

As shown in Figure 3, several anti-influenza virus drugs have been developed. However, their efficacy is limited due to side effects on the biological system [11] and the frequent appearance of resistant strains [12-14]. In addition, most of the viruses that have been circulating so far have amantadine resistance [15, 16]. Pandemics have occurred many times in the past, and it is feared that epidemics will continue to spread around the world in the future.

Phytochemicals, which are contained in food and are non-nutrients, are known to exhibit various functionalities [17-19], and several research have been reported showing that they inhibit the growth of DNA viruses and RNA viruses [20]. The efficacy of foods, food extracts and ingredients has also been reported in anti-influenza virus strategies [21-24]. Polyphenols, which are part of phytochemicals, have multiple phenolic hydroxyl groups in their molecular structure, and are metabolized within plants. It is known to be a functional ingredient contained in, and many types have been discovered depending on its structure. It is very interesting because its functionality also depends on the structure of the flavonoids.

In this doctoral thesis, while screening *cucurbitaceous* foods, I focused on the strong anti-influenza virus activity of wild watermelon juice (WWMJ) and aimed to investigate the inhibition mechanism and the relationship between the anti-influenza virus activity of natural compounds (especially, flavonoids and prenylated flavonoids) and their

component structures. The project objectives are as follows.

In Chapter I, I screened *cucurbitaceous* foods with anti-influenza virus effects, and found various anti-influenza virus effects of WWMJ. In other words, the efficacy against influenza A and B virus strains, including clinical isolates and drug-resistant strains, were evaluated in a cultured cell system (*in vitro*), and intranasal administration of WWMJ was performed in an animal model of influenza A virus infection (*in vivo*).

In Chapter II, metabolomic analysis was performed to detect the active ingredients of WWMJ, and a comprehensive analysis of functional components was performed. As a result, it was found that various polyphenols were contained. Based on the obtained results, I focused on the anti-influenza virus effects of flavonoids and discussed them from the viewpoint of molecular structure. The anti-influenza virus effects of flavonoids depend on their molecular structure, and large differences in activity were confirmed even within the same flavonoid group.

In Chapter III, I focused on the dramatic increase in anti-influenza virus activity by intramolecular modification (prenylation) of flavonoids. To investigate the effect of substituents in the naringenin molecule on the anti-influenza effect, derivatives with prenyl groups and similar modified groups were synthesized and the antiviral activity and intracellular uptake of known and novel naringenin derivatives were evaluated.

Chapter I

Juice of *Citrullus lanatus* var. *citroides* (wild watermelon) inhibits the entry and propagation of influenza viruses *in vitro* and *in vivo*

1.1. Introduction

Influenza cases continue to be reported, even as other infectious diseases continue to be prevalent [25, 26]. Influenza viruses A and B are known to cause seasonal epidemics, and in 2009, the rapid spread of the A strain (A/H1N1) caused a global pandemic [27]. The epidemic of infection is caused by antigenic mutation of RNA virus, and there are reports of human infection with avian influenza virus [28], and the emergence of new viruses with drug resistance [13-15]. Newly isolated influenza D viruses from animals [3, 29] have been reported to infect human bronchial epithelial cells [30]. Therefore, it has the potential to be a zoonotic infection. Furthermore, in Japan, where the birthrate is declining and the population is aging, influenza virus infections have become recognized as a serious health risk, there is an urgent need to develop preventive and therapeutic methods from a new perspective.

To solve these problems, I focused on the functionality of food in view of its ability to respond quickly to resistant viruses and its high safety to humans. Currently, various food extracts and functional ingredients have been reported to be useful to the body, and their functionality is diverse [31-33], foods that are effective against influenza virus have also been reported [21-24, 34].

Our research group reported that adlay tea and its constituents and functional ingredients are effective against influenza viruses and continue to report effective food extracts and

foods [35-37] (Figure 1-1). While scrutinizing many food extracts, this study focused on the anti-influenza virus activity of *Cucurbitaceous* foods. I focused on the anti-influenza virus effect of wild watermelon (WWM), which showed strong inhibitory activity.

Figure 1-1. Anti-influenza virus foods

The left shows the previous research [Reference 21-24], and the right shows the report of our research group [Reference 35-37].

WWM (*Citrullus lanatus* var. *citroides*) is a plant native to the Kalahari Desert in southern Africa (Figure 1-2), due to its high-water content, it is valued locally as a source of water, and the seeds of the same species, *Citrullus ecirrhosus*, contain many minerals and essential amino acids [38], and are also treated as a valuable source of nutrients. In addition, it has high antioxidant capacity [39], and can grow even under environmental stress conditions such as extreme dryness and high ultraviolet rays. This is thought to be caused by specific components (proteins and genes) [40]. Companies that have paid attention to such functionality are cultivating it in Japan, but its recognition is still low. It is also a relatively new subject of research in antiviral strategies. In this chapter, I have investigated the anti-influenza activity of WWM in A/PR/8/34-infected MDCK cells and BALB/c mice.
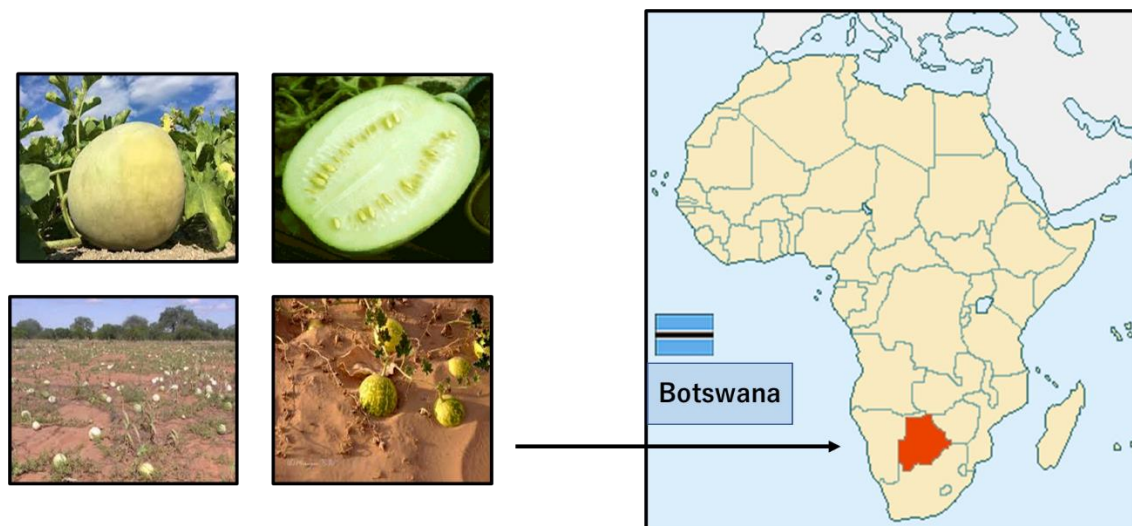
Figure 1-2. Wild watermelon (*Citrullus lanatus* var. *citroides*) and country of origin

Located in Botswana in Southern Africa, it is native to the Kalahari Desert, which has the lowest annual rainfall.

1.2. Materials and Methods

1.2.1. Cell lines and viruses

Madin–Darby canine kidney (MDCK) cells were grown in Eagle's minimum essential medium (E-MEM; Wako Pure Chemical Industries, Ltd) containing 7% fetal bovine serum (FBS). Monkey kidney (CV-1) cells were cultured in Dulbecco's modified Eagle's medium (DMEM; Wako) containing 10% FBS. Type A influenza viruses H1N1 (A/Puerto Rico/8/34, A/New Caledonia/20/99, A/Beijing/262/95, A/Suita/6/2007, A/Suita/114/2011, A/Osaka/2024/2009, A/Osaka/71/2011) and H3N2 (A/Sydney/5/97, A/Suita/120/2011) and type B influenza viruses (B/Nagasaki/1/87, B/Shanghai/261/2002) were used in the experiments. The virus culture was diluted in serum-free MEM containing 0.04% bovine serum albumin (BSA, fraction V; Sigma-Aldrich) and then incubated with the cells to infect them at a multiplicity of infection (MOI) of 0.001 for 1 h at 37°C. The medium was then removed and replaced with serum-free DMEM containing 0.4% BSA and 2 μg/ml acetyl trypsin (Merck Sigma-Aldrich) for the rest of the infection period. The cells and

virus strain were provided by the Research Institute for Microbial Diseases of Osaka University (Suita, Osaka, Japan), and Osaka strains were provided by the Osaka Prefectural Institute of Public Health (now, known as Osaka Institute of Public Health) following appropriate measures (Osaka, Japan).

1.2.2. Preparation of watermelon extracts and other sample extracts

Wild watermelon and the juice from commercially available watermelon (WM) were tested for their anti-influenza activity in this study. WWMJ was provided by Euglena, Co., Ltd. WWMJ was treated at 80°C for 30 min, and the proteins were removed to establish if lectins participated in the antiviral activity. WMJ was squeezed from watermelon obtained from a Hitorijime cultivar produced in Kumamoto and purchased from a supermarket. WWMJ and WMJ were centrifuged at 1,600 ×g and the supernatants freeze-dried. The dry weight of each resulting powder was measured and then dissolved in 20 mg/ml of ultrapure water. The samples were then sterilized by filtration through a Millex GX membrane with a 24 mm diameter and a pore size of 0.45 μm (Merck Millipore) and stored at − 30°C until analysis. Other sample foods of *Cucurbitaceae*, pumpkin (*Cucurbita moschata*) and zucchini (*Cucurbita pepo* L.), were purchased from a supermarket (Figure 1-3). The samples were cut and freeze-dried. Next, the dried samples (5 g) were powdered, mixed with water (50 ml), and extracted in a hot water bath for 60 min at 80°C. Subsequent steps after the centrifugation were the same as described above.

1. **Pumpkin** (*Cucurbita moschata*)

2. **Zucchini** （*Cucurbita pepo* L.）

3. **Watermelon** （*Citrullus lanatus* M.）

4. **Wild watermelon**　（*Citrullus lanatus* var. *citroides*）

Figure 1-3. Preparation of *Cucurbitaceae* samples

Cucurbitaceous foods were squeezed and extracted. The juices (3 and 4) were processed and used as a sample for the screening test. Wild watermelon juice was provided by Euglena Co. Ltd, and other foods were purchased from supermarkets.

1.2.3. Viral yield determination in the presence of watermelon samples

The effects of the addition of food samples on viral yield were determined using a modified version of the previously described procedure [35] (Figure 1-4). MDCK cells were cultured in a 24-well plate (Thermo Fisher Scientific) at 1×10^5 cells/well in 500 μl/well MEM containing 7% FBS and incubated for 24 h at 37°C. The confluent monolayers of cells were then rinsed twice with serum-free MEM. Diluted virus culture was incubated with the cells at a MOI of 0.001 for 1 h at 37°C. The infected cells were rinsed once with serum-free MEM after 1 h and then cultured in DMEM containing extract (500 μl/well). Supernatants were collected after 24 h as the influenza virus samples and used in a focus-forming reduction assay.
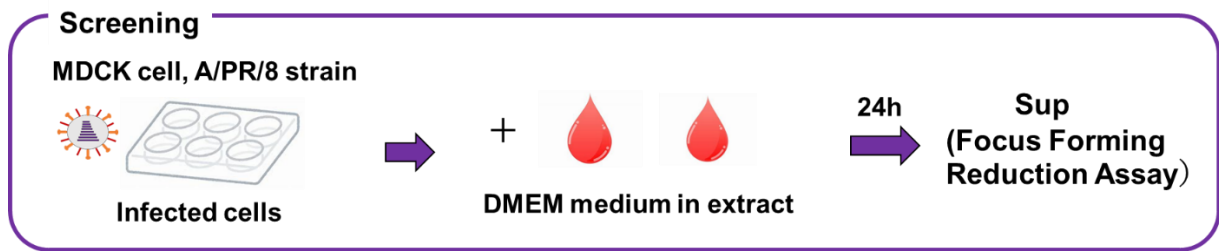
Figure 1-4. Screening assay

The monolayer cultured MDCK cells were infected with A/PR/8/34 strain at 0.001 moi and cultured for 24 hours in the DMEM medium containing the sample. After 24 hours, supernatants were collected. Collected samples were subjected by FFRA.

1.2.4. Focus-forming reduction assay (FFRA) of viral activity

The FFRA was performed according to a slightly modified version of the previously described method [35, 41]. MDCK cells (approximately 10^4 cells/well) were seeded in 96-well flatbottom plates (Corning Inc.) and incubated in 5% CO_2 at 37°C to form monolayers. The viral solutions were serially diluted 10-fold in 96-well round-bottom plates (Thermo Fisher Scientific) in MEM containing 0.04% BSA on the following day. MDCK cells in 96-well flat-bottom plates were washed twice with serum-free MEM and then 30 μl of each viral mixture was added to each well. Samples were incubated for 1 h at 37°C. The viral solutions were then removed and cells were washed with serum-free MEM, covered with 100 μl of MEM mixture (equal volumes of FBS-free MEM and Avicel® RC-591 NF; FMC Health & Nutrition) containing 0.04% BSA, and incubated for 18 h at 37°C. The supernatant was then removed, and cells were washed with serum-free MEM and fixed with absolute ethanol at room temperature for 10 min. The ethanol was then removed completely. Cells that were not stained immediately were stored at −80°C until staining. Focus staining was performed by adding 50 μl of murine monoclonal anti-HA antibody [C179 for A (H1N1) viruses [42], F49 for A (H3N2) viruses [43], and 7B11 for B viruses [44], and a goat anti-mouse IgG antibody conjugated to

horseradish peroxidase (Merck KGaA). The peroxidase reaction was developed for 30 min according to the procedure given by Graham and Karnovsky [45], using 0.1% H_2O_2 and 0.3 mg/ml 3,3′-diaminobenzidine tetrahydrochloride (Wako) in phosphate-buffered saline (PBS). Cells were rinsed with water and dried with a hair dryer after the reaction. The numbers of foci in immunostained infected cells were determined under an inverted light microscope (Figure 1-5).
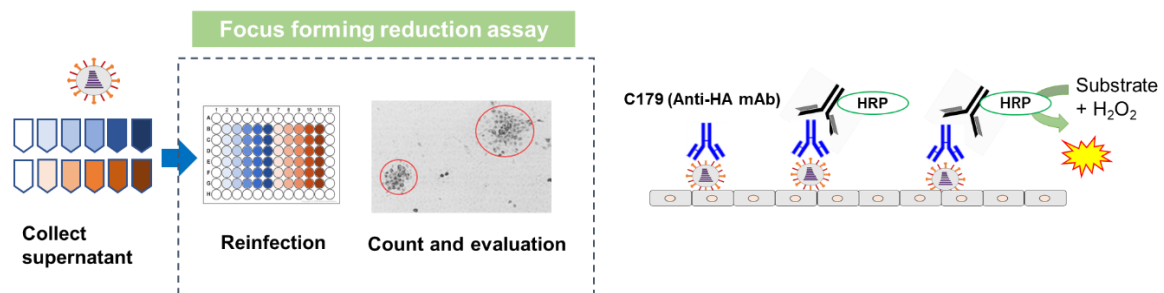
**Figure 1-5. Focus forming reduction assay and staining**

The monolayer-cultured MDCK was reinfected with A/PR/8/34 in supernatant and cultured for 18 hours in the serum-free MEM medium containing Avicel. After, infected cells were fixed with ethanol and immunostained using HA or other viral protein monoclonal antibody.

1.2.5. Time-of-addition assay

A time-of-addition assay was performed using a modified version of the previously described procedure [35]. MDCK cells were plated in 24-well plates as described above, rinsed twice with serum free MEM, and then inoculated with A/PR/8/34 (MOI = 0.01). Cells were rinsed twice with serum-free MEM and incubated in DMEM after 1 h as described above. DMEM containing 1 mg/ml WWMJ, which is approximately 10 times the median inhibitory concentration (IC_{50}), was added at different time points: within the 12 h period prior to infection (-12– -1 h, pretreatment), between 1 h prior to infection and time of infection (-1–0 h, adsorption), and between 0–2 h, 2–4 h, 4–6 h, 6–8 h, or 0–8 h after infection (replication), as shown in Figure 1-6. Cell monolayers were rinsed twice

with serum-free MEM after each incubation period and the medium was replaced with fresh medium. Cells were cultured for 8 h after infection. Infected cells were then frozen at $-80°C$ and subjected to two freeze–thaw cycles before the viral yield were determined with the focus-forming assay.
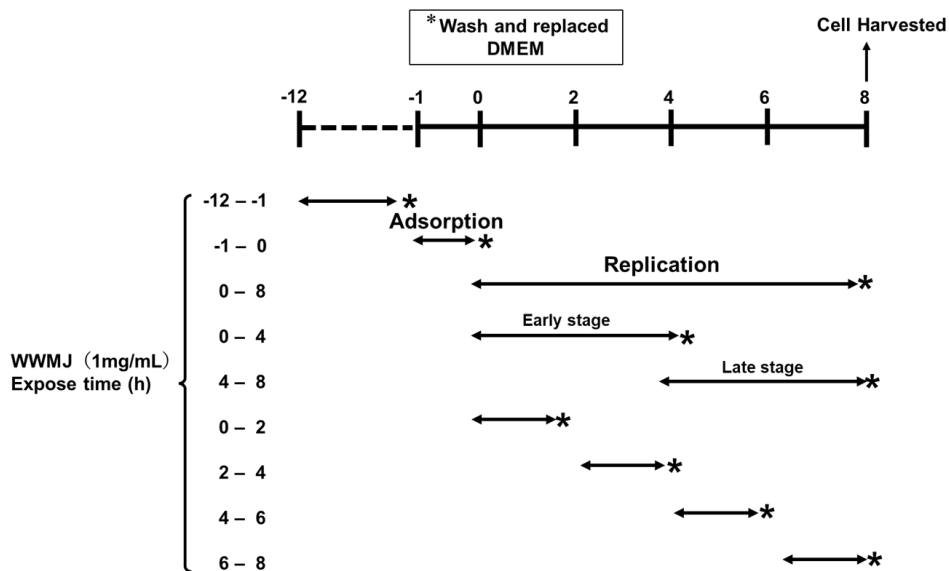
Figure 1-6. Time schedule of time-of- addition assay

DMEM medium containing WWMJ was exposed at times before and after infection. After exposure, the cells were washed several times with MEM medium and replaced with DMEM medium. Cells were then harvested by pipetting and virus in the supernatant was evaluated.

1.2.6. Cell viability determination

Cell viability was determined with a Cell Proliferation Kit I (MTT) (F. Hoffmann–La Roche Ltd). The cytopathic effects in the virus infected cells to which various concentrations of WWMJ had been added were observed under a microscope.

1.2.7. HI test

The HI test was conducted using receptor-destroying enzyme treated guinea-pig red blood cells in 96-well U-bottom plates (Thermo Fisher Scientific) with the standard microtiter assay as described previously [46] (Figure 1-7).

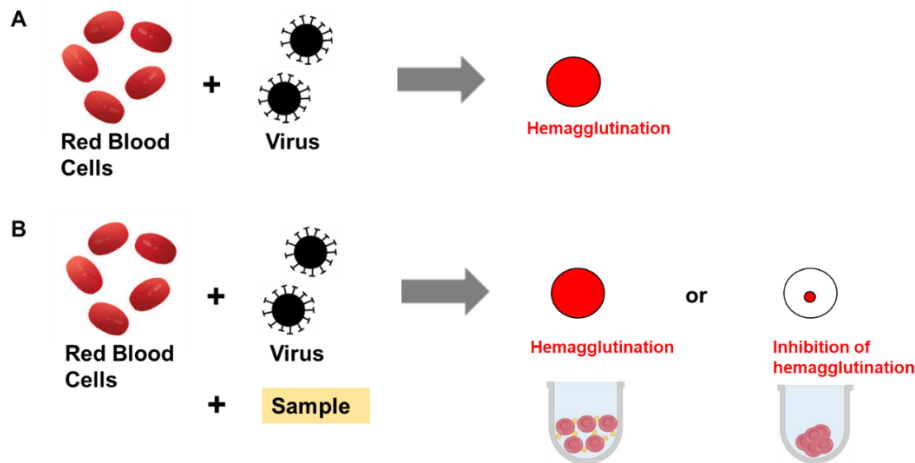

Figure 1-7. Hemagglutination inhibition (HI) test

1.2.8. Viral adsorption inhibition assay

The amount of virus attached to the cells was determined by measuring the viral RNA encoding the M protein (MP). Viral RNA bound to cells was extracted, and cDNA synthesized, and viral RNA quantified as described previously [35] (Figure 1-8).
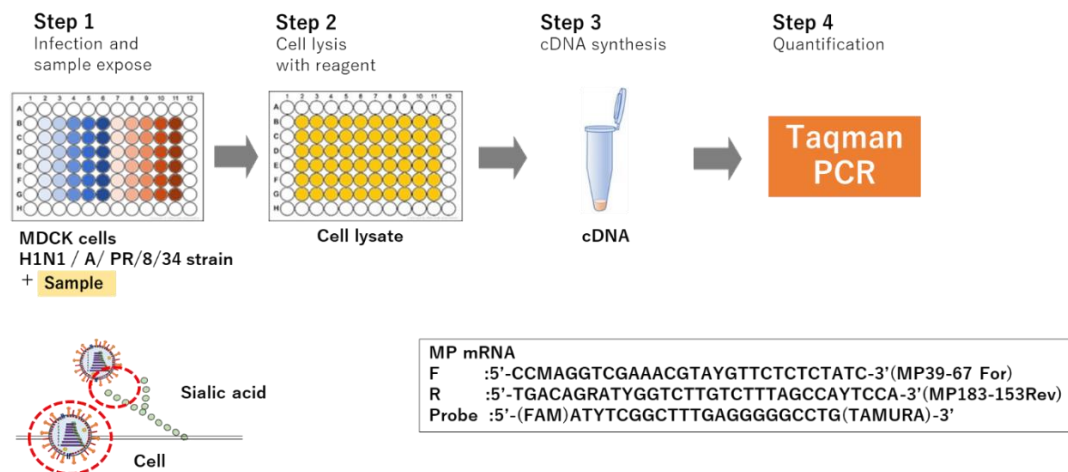

Figure 1-8. Viral adsorption inhibition assay

1.2.9. Cell fusion inhibition test

Cell–cell fusion was analyzed using the method previously described [35]. Briefly, the influenza virus solution (A/ PR/8/34: MOI of 0.001) was added to CV-1 cells and cultured for 24 hr. Infected cells were washed twice and incubated for 15 min in DMEM containing 10 µg/ml trypsin. Cells were washed twice and incubated for 30 min in DMEM containing 1 mg/ml WWMJ. Next, cells were washed and treated with fusion medium to adjust the pH to 5.0 and incubated for 2 min. Thereafter, cells were washed twice and incubated for 3 h with DMEM containing 2% FBS. Cells were then stained with Giemsa and the number of fused cells counted (Figure 1-9).
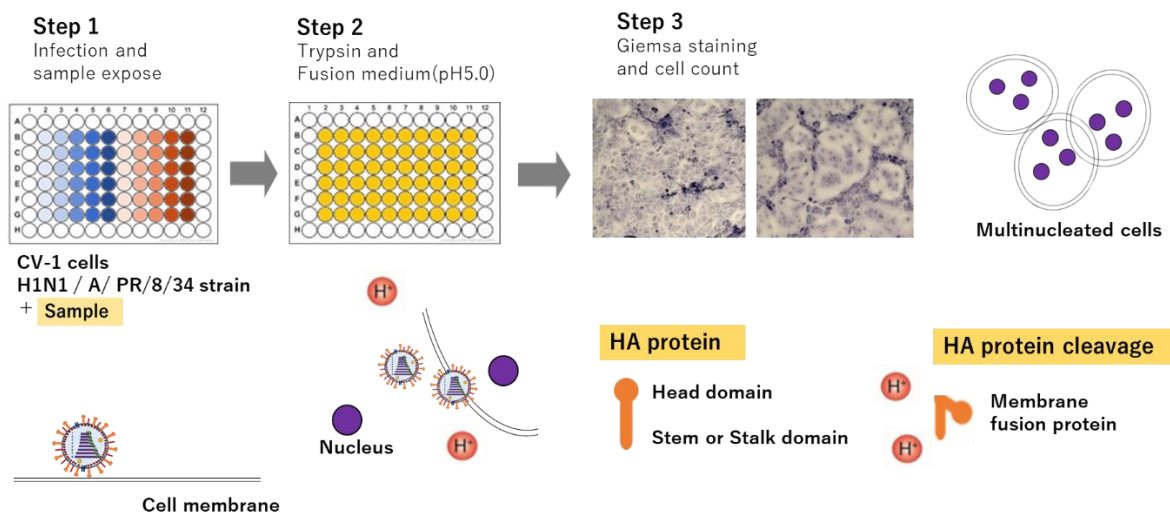
Figure 1-9. Cell fusion inhibition test

1.2.10. Mice and infection experiment

Five-week-old female BALB/c mice (20–22g) were obtained from Charles River Laboratories International, Inc. Mice were maintained in a laminar flow hood at the Animal Experiment Facility of the Hyogo College of Medicine, Hyogo, Japan, under suitable conditions (12-h light/dark cycle, temperature 25°C, relative humidity 50%) and fed AIN-76 purified mouse diet (CLEA Japan, Inc.) for 1 week. Mice were divided into two groups (test group and control group) containing 10 mice each. One day prior to

infection, 20 µl of WWMJ (20 mg/kg/day) was inoculated into one nostril of the 6-week-old mice in the test group; the control group was given an equal volume of PBS. On the following day, mice were infected with 100 FFU/ mouse of A/PR/8/34 influenza virus, a mouse-adapted strain, by inoculating 20 µl of the virus solution into one nostril. WWMJ (20 µl) was inoculated nasally into the sample group and 20 µl of PBS into the control group after 1 h of virus inoculation. WWMJ and PBS treatments were repeated daily for the next 3 days. Body weights and survival rates of the WWMJ- and PBS-treated mice were determined. Survival was monitored for 14 days after infection (Figure 1-10). Animal husbandry was performed in accordance with the ordinance of the regulation for Enforcement of the Act on Welfare and Management of Animals relating to the care and management of experimental animals (Ordinance, 2016).

This study was performed with the approval of the Animal Experiment Committee of Hyogo College of Medicine, Nishinomiya, Japan (approval number: 15–007) and complied with the ordinance of the Regulation for Enforcement of the Act on Welfare and Management of Animals relating to the care and management of experimental animals.
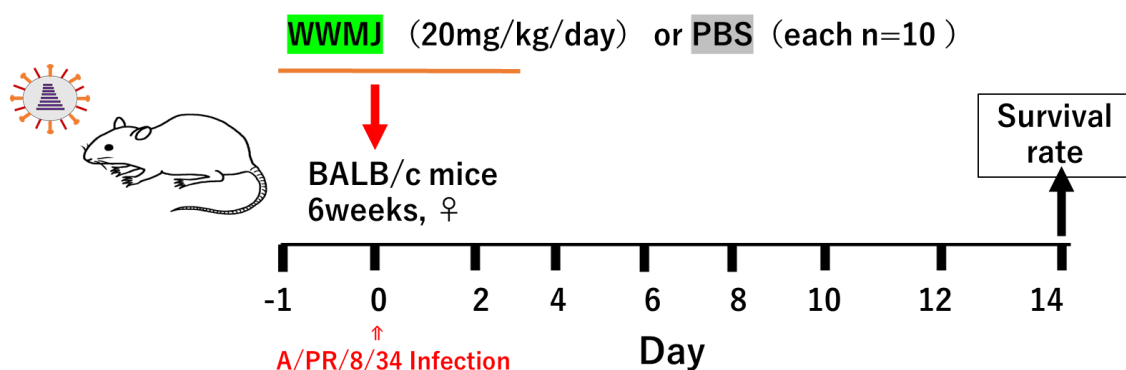
Figure 1-10. Mice and infection experiment schedule

In vivo experiment schedule.

1.2.11. Statistical analyses

The amounts of virus determined in the time-of-addition assay and the antiviral assay were analyzed by the Student's t-test in Excel Toukei version 6.0 (Esumi). The survival rates of the virus infected and virus infected-WWMJ treated mice were analyzed by the Kaplan–Meier method and logrank test in Excel Toukei Statcel 3 (OMS). A p-value $p <$ 0.05 was considered statistically significant. Values are presented as means ± standard deviations (SD).

1.3. Results

1.3.1. WWMJ inhibits influenza viral growth

The viral growth in infected MDCK cells treated with WWMJ and WMJ (squeezed from a commercially available WM) was compared. WWMJ inhibited the proliferation of the influenza virus within cells in a concentration-dependent manner (Figure 1-11), but WMJ did not cause viral inhibition (Data not shown). The IC_{50} of WWMJ was 0.11 mg/ml. The MTT test revealed that WWMJ was not cytotoxic to MDCK cells. Notably, 1 mg/ml WWMJ reduced the virus by 80% – 90% as compared to control cells lacking WWMJ. The IC_{50} values of pumpkin and zucchini were 1.07 and 0.74 mg/ml, respectively (Table 1-1). WWMJ had the highest viral growth inhibition activity among plants of *Cucurbitaceae*.
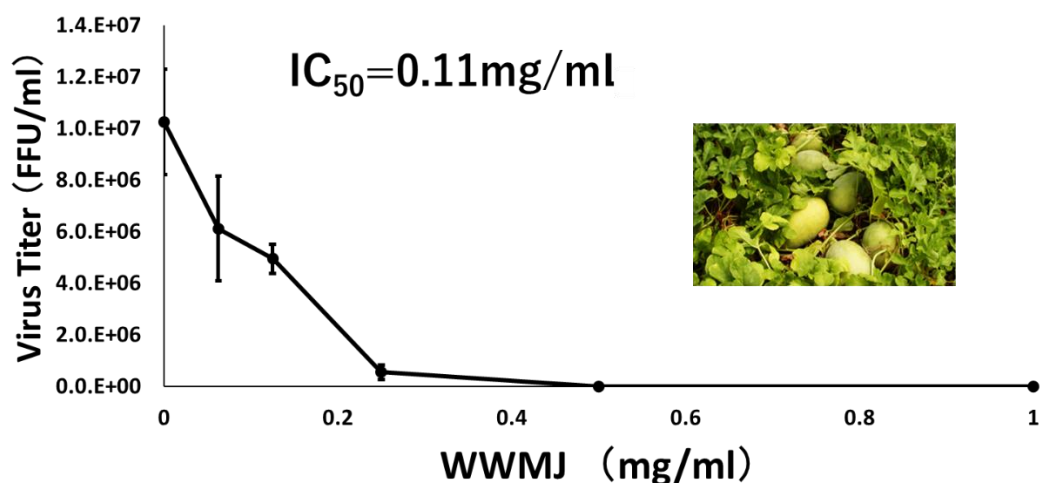
Figure 1-11. WWMJ inhibits influenza A viral growth

DMEM medium containing WWMJ was exposed at times before and after infection. After exposure, the cells were washed several times with MEM medium and replaced with DMEM medium. Cells were then harvested by pipetting and virus in the supernatant was evaluated.

Table 1-1. Anti-influenza virus activity of Cucurbitaceae

ND: Not detected

Food extract	Scientific name	IC_{50} (mg/ml)
Pumpkin	(*Cucurbita moschata*)	1.07
Zucchini	(*Cucurbita pepo* L.)	0.74
Watermelon	(*Citrullus lanatus* M.)	ND

1.3.2. Antiviral effects of WWMJ against various type A and B influenza viruses

The antiviral effects of WWMJ on various influenza strains were then investigated. Table 1-2 shows the IC_{50} values of WWMJ for various influenza viral strains. WWMJ inhibited the growth of type A and B influenza viruses. IC_{50} values were found to be 0.11–0.20 mg/ml for H1N1, 0.71, 0.87 mg/ml for H3N2, and 0.41, 0.88 mg/ml for type B viruses. There was no significant difference in the IC_{50} values between the H1N1 viruses. WWMJ

18

also showed similar inhibitory activities against the oseltamivir-resistant (A/Osaka/2024/2009 and A/Osaka/71/2011) and sensitive strains (A/PR/8/34, A/New Caledonia/20/99, A/Beijing/262/95, A/Suita/6/2007, and A/Suita/114/2011), for which the IC_{50} values were found to be similar.

Table 1-2. Effect of WWMJ on the multiplication of various influenza virus types and strains

Values are the average of results obtained using various final concentrations of WWMJ and MDCK cells, from three independent experiments. [a]The IC_{50} of WWMJ and that of oseltamivir acid [Reference 13] are given in mg/ml and ng/ml, respectively. Values are the average of results obtained using various final concentrations of WWMJ and MDCK cells, from three independent experiments. [b] The CC_{50} of WWMJ and that of oseltamivir acid [Reference 13] are given in mg/ml and ng/ml, respectively. [c] Selectivity index = CC_{50}/IC_{50}. [d] Oseltamivir-resistant virus strain.

ND: not detected.

Virus type and strain	IC_{50}[a] (mg/ml)	(ng/ml)	CC_{50}[b] (mg/ml)	(ng/ml)	SI[c]	
	WWMJ	Oseltamivir acid	WWMJ	Oseltamivir acid	WWMJ	Oseltamivir acid
A (H1N1)						
PR/8/34	0.11 ± 0.05	0.45 ± 0.01	>10	>200	>100	>444,444
New Caledonia/20/99	0.20 ± 0.03	0.38 ± 0.18	>10	>200	>50	>526,315
Beijing/262/95	0.11 ± 0.03	ND	>10	ND	>90	ND
Suita/6/2007	0.14 ± 0.03	ND	>10	ND	>71	ND
Suita/114/2011	0.19 ± 0.08	ND	>10	ND	>52	ND
Osaka/2024/2009 [d]	0.13 ± 0.01	180 ± 59	>10	>200	>76	>1,111
Osaka/71/2011 [d]	0.20 ± 0.03	259 ± 75	>10	>200	>50	>772
A (H3N2)						
Sydney/5/97	0.87 ± 0.07	ND	>10	ND	>11	ND
Suita/120/2011	0.71 ± 0.02	ND	>10	ND	>14	ND
B						
Nagasaki/1/87	0.88 ± 0.25	6.10 ± 1.19	>10	>200	>11	>32,786
Shanghai/261/2002	0.41 ± 0.06	ND	>10	ND	>24	ND

1.3.3. Influenza growth stage inhibited by WWMJ

The stage at which viral growth is inhibited by WWMJ was determined by performing a time-of-addition assay. The time points at which WWMJ was added to the incubation mixture are shown in Figure 1-6. One cycle of viral (A/PR/8/34) proliferation within a cell takes 8 h as reported previously [35, 47]. Based on this information, Figure 1-12 shows the stages of viral multiplication that were inhibited by WWMJ. The exposure

period during viral replication was then divided into 2h intervals; the results obtained showed that WWMJ inhibited two different steps in the viral infection process. The first step was the adsorption of the virus onto the cells (-1–0 h of viral infection) and the second was in the late stage of viral replication (4–8 h after viral infection), especially the period associated with viral particles assembly (6–8 h after viral infection). Since WWMJ inhibited the adsorption of the virus onto the cells, the inhibitory mechanism at this step was then elucidated. Type I high mannose- specific antiviral algal lectins have been reported to bind with high affinity to the viral envelope HA [48]. The presence of similar lectins in WWMJ was determined by performing a viral yield assay in MDCK cells using heat-treated WWMJ, which showed that the virus-inhibiting activity of WWMJ was not affected even after heat treatment.
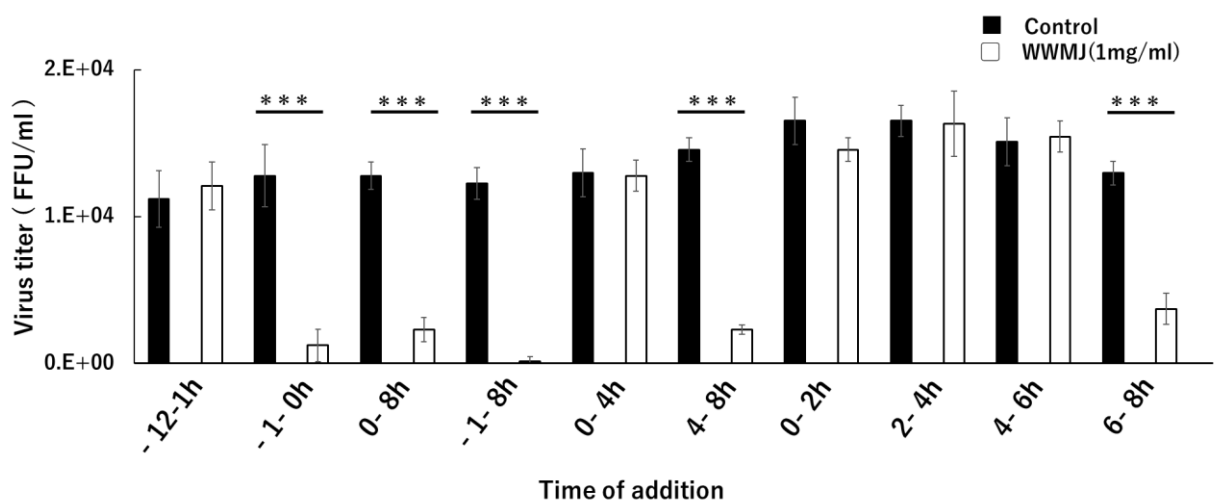
**Figure 1-12. Effect of WWMJ on viral growth stage and virus titer**

Time points and exposure periods of addition of WWMJ to MDCK cells infected with influenza virus A/PR/8/34. FFRA-assay results indicated by open columns representing viral yields of control cells and closed columns representing viral yields of cells treated with WWMJ. Data are representative of three independent experiments. ***$p < 0.01$

1.3.4. WWMJ inhibits the cellular entry of influenza virus

WWMJ inhibits viral adsorption onto cells as shown in Figure 1-12. It was confirmed by the HI test. This test showed that 4 mg/ml WWMJ reacted weakly with the A/PR/8/34 virus (Figure 1-13-a). However, the adsorption inhibition assay showed that WWMJ significantly inhibited the adsorption of influenza virus onto MDCK cells at 37°C, in a WWMJ-concentration-dependent manner (Figure 1-14). The time-of-addition assay showed that WWMJ (1 mg/ml) reduced viral adsorption with an inhibition ratio of 0.903 (Figure 1-12), and although no inhibition of viral binding occurred in the presence of WWMJ at 4°C, 10 mg/ml WWMJ reduced the viral binding with the cells at 37°C, with an inhibition ratio of 0.648 (Figure 1-14). The inhibition ratio was defined as $(A - B)/A \times 100$, where A represents the amount of virus in the mock-treated cells and B represents the amount of virus in the WWMJ-treated cells. Viral adsorption was analyzed by the time-of-addition assay at 37°C since this step could comprise both the attachment of the virus to the cells and virus internalization, such as by endocytosis. However, the viral adsorption assay showed that the amount of bound virus at 37°C was 10 times higher than that at 4°C. WWMJ did not suppress cell–cell fusion using the A/PR/8/34 virus and CV-1 cell at any of the concentrations tested (up to 4 mg/ml), and the fusion index was found to be more than 0.85 at every concentration (Figure 1-13-b). These results suggested that WWMJ inhibited viral entry by endocytosis but did not inhibit viral fusion ability.
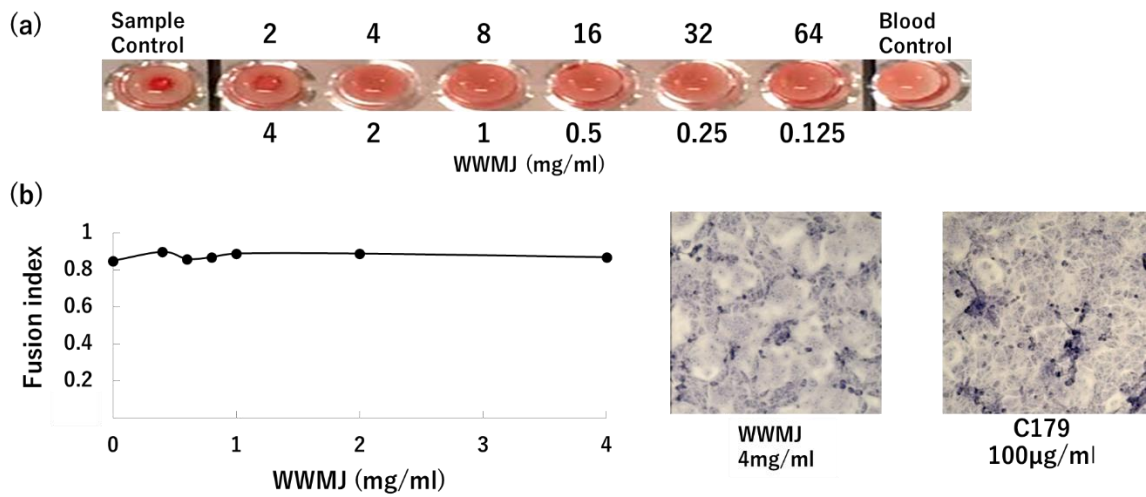
Figure 1-13. Effects of WWMJ on viral adsorption

(a) HI assay. "Sample control" represents red blood cells incubated with WWMJ and "Blood control" represents red blood cells infected with virus. Top numbers represent the HI titers and bottom numbers represent the WWMJ concentrations (mg/ml). (b) Fusion inhibition assay. The fusion index $= 1 - ($ number of cells/number of nuclei). Data are representative of two independent experiments.
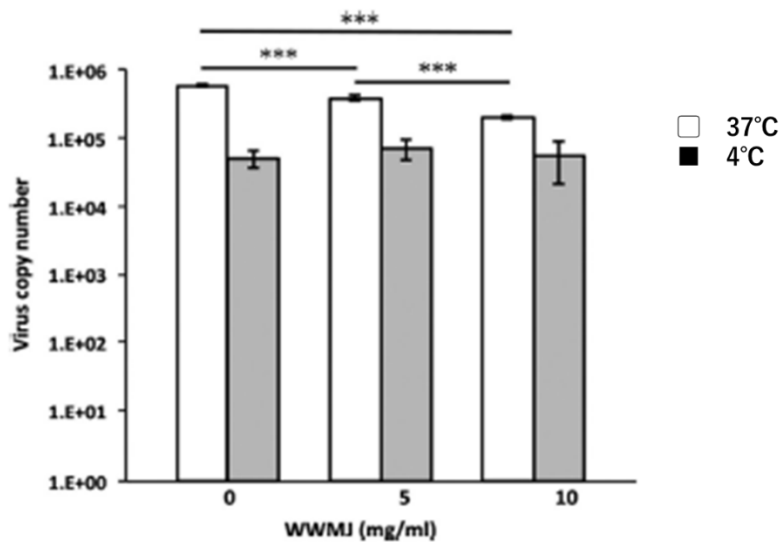

Figure 1-14. Effect of WWMJ on viral binding to cells

White columns indicate the viral adsorption onto cells at 37°C at three different concentrations of WWMJ. Gray columns indicate the same at 4°C. Error bars indicate SD (n = 3). Data are representative of three independent experiments. ***$p < 0.01$

1.3.5. Effects of WWMJ treatment on influenza virus-infected mice

The therapeutic effects of These WWMJ *in vivo* were investigated using a mouse model of influenza viral infection. The experimental schedule is shown in Figure 1-10. Mice were treated with 20 mg/kg/day WWMJ (test group) or PBS (control group), and their survival rates were evaluated (Figure 1-15). The body weights of the WWMJ-treated and control mice did not show any significant difference (data not shown). As shown in Figure 1-15, the nasal administration of WWMJ slightly improved the survival rate of the infected mice monitored for 14-day post inoculation. WWMJ-treated mice were found to die 6-day post inoculation, as compared to death 4-day post inoculation observed with control mice. The survival rates of the WWMJ-treated mice were 90 and 50 at 6- and 7-day post inoculation, respectively, as compared to 20 and 0, respectively, in the control mice. Thus, WWMJ treatment increased the lifespans of influenza virus-infected mice by at least 2 to 3 days. Kaplan–Meier method and log-rank test showed that this difference in survival was significant.
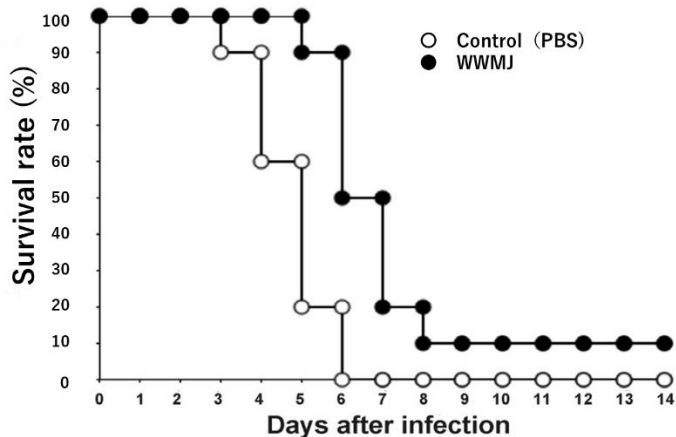
Figure 1-15. *In vivo* effect of WWMJ on infected mice

Survival rates of BALB/c mice (6 weeks old) infected with mouse-adapted influenza virus strain A/PR/8/34 at 100 FFU/mouse by nasal mucosal administration for a 14-day period are shown. Control group treated with PBS, open circles ($n = 10$ mice); WWMJ group, filled circles ($n = 10$). Log-rank test showed that this difference in survival was significant ($p < 0.05$)

1.4. Discussion

Influenza is an acute respiratory disease that affects many people throughout the world. Several anti-influenza drugs are used to treat patients infected with various influenza viruses. However, viral strains resistant to these drugs have been reported [49, 50]. The anti-influenza efficacy of WWMJ in A/PR/8/34-infected MDCK cells was evaluated in this study. WWMJ was found to be the strongest inhibitor of the growth of influenza virus in MDCK cells among all the screened plant extracts of *Cucurbitaceae*. WWMJ inhibited the proliferation of the influenza virus within the cells in a concentration-dependent manner, while WMJ did not inhibit the virus. Viral infections are inhibited by carbohydrates, such as the marine-microalga-derived sulfated polysaccharide p-KG03 [51]. The sugar contents of WWMJ and WMJ were determined and found to be 2°Bx and 8°Bx, respectively, on the Brix scale; however, neither contained sulfated polysaccharides (data not shown). WMJ was found to have 4 times the sugar content of WWMJ, which indicates that the antiviral effect of WWMJ is not attributable to the influence of sugar. Figure 1-13 shows that WWMJ did not inhibit the recognition of sialic acid on the cell membrane by HA protein. As a conclusion, Figure 1-14 suggests that WWMJ inhibits energy-dependent entry of viruses, in other words, endocytosis. The finding that WWMJ has a strong anti-influenza activity, whereas the commercially available WMJ has little anti-influenza activity, implies that watermelons have lost their effective antiviral components over the course of breeding to suit our taste. Consistent with this idea, it has been reported that wild plants have anti-influenza properties [52]. Therefore, wild plants such as WWM and various other spices may have strong antiviral activities against influenza viruses. In this chapter, further experiments were carried out to clarify the mechanism and stage of the anti-influenza activity of WWMJ. Figure 1-12 shows that

WWMJ inhibits adsorption (or entry) and late phase of influenza virus propagation in infected cells. The results of Figures 1-12 and 1-14 suggested that clathrin-dependent and/or -independent endocytosis [53] might be inhibited by WWMJ. Inhibition of the late phase of influenza virus propagation might involve inhibition of viral assembly, and the mechanism might be like the inhibition mechanism of daidzein [54]. The assessment of the effect of WWMJ on various virus strains showed that WWMJ inhibited the growth of type A and B influenza viruses. However, no significant difference in IC_{50} values was found between H1N1 viruses. Although IC_{50} values of H1N1 viruses were significantly 2- to 4-times lower than those of H3N2 and type B viruses, no significant difference was found between the IC_{50} values for H3N2 and type B viruses, indicating that WWMJ possesses stronger antiviral activity than adlay tea [35]. Therefore, the viral replication-inhibition activity of WWMJ does not show virus type specificity, unlike that of amantadine [49]. WWMJ also showed similar inhibitory activities against the oseltamivir-resistant (A/Osaka/2024/2009 and A/Osaka/71/2011) and sensitive strains (A/PR/8/34, A/New Caledonia/20/99, A/Beijing/262/95, A/Suita/6/2007, and A/Suita/114/2011), which had similar IC_{50} values, suggesting that the effective component(s) in WWMJ that inhibit viral growth act differently from the inhibitory components of oseltamivir. Moreover, since WWMJ shows similar effectiveness in inhibiting both type A and B influenza virus growth (Table 1-2), WWMJ might have utility as a new preventive and/or therapeutic substance, which can combat the problem of emergence of mutated drug-resistant strains. The time-of-addition assay showed that WWMJ inhibited viral adsorption and late viral replication, indicating that it may contain two or more components that act as the main inhibitors of viral adsorption and assembly. The findings of this study indicate that WWMJ might have potential utility as a novel alternate

treatment for influenza virus, although further biochemical and molecular biological studies are required to further understand its active components and antiviral mechanisms. WWMJ was found to reduce the viral titer *in vitro* and improve the survival of influenza virus-infected mice *in vivo*. The results obtained in this study therefore demonstrate an alternate mode of management and treatment of influenza infections that may be useful for combating the virus. Thus, this study might have proved the candidature of WWMJ as a potentially novel and alternate mode of treatment for influenza infection. Since WWMJ has been indicated to comprise multiple antiviral components, this alternate mode of treatment can ensure the prevention of new resistant viral strains. This alternate mode of treatment promises to be nonspecific to viral strains, thereby resulting in a therapeutic option for infections caused by newly emerging mutated influenza virus strains as well.

Chapter II

Anti-influenza A virus activity of flavonoids *in vitro*: a structure-activity relationship

2.1. Introduction

Synthetic chemical substances such as oseltamivir and favipiravir have been confirmed the high growth inhibitory effect against influenza viruses, but side effects have also been reported. On the other hand, natural chemical substances in plants are attracting attention, natural chemicals have potential as materials for new therapeutic agents.

Flavonoids are a type of polyphenol, common natural organic compounds. There are classified into various groups, such as flavone, isoflavone, flavonol, flavanone, and flavan-3-ol etc, based on their chemical structure (Figure 2-1).
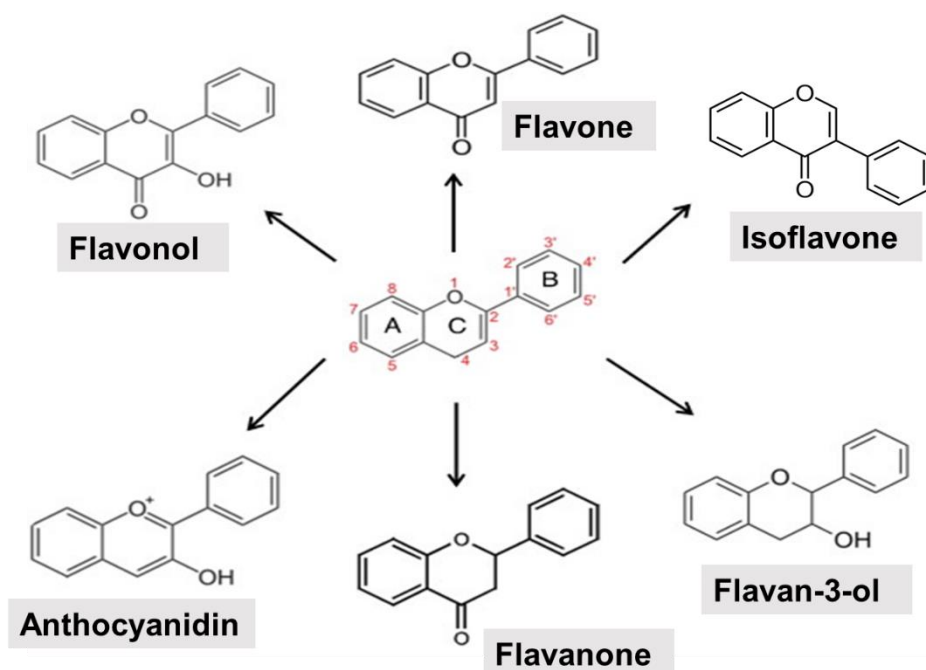

Figure 2-1. Flavonoids and their structure

Our research group previously reported that the anti-influenza virus activity of daidzein, umbelliferone, herniarin, quercetin, luteolin, and caffeic acid in food extracts [36, 37] (Figure 2-2). Interestingly, the antiviral activity of compounds for MDCK cells differed owing to the presence of different functional groups. Studies on the relationship between the type of modifying group patterns and function of catechins have revealed the mechanisms underlying their effect against influenza virus infection [55-58]. However, only a few studies have comprehensively explored other flavonoid compounds for use in novel therapeutic strategies. Previous studies suggested that WWMJ contains many polyphenols. Therefore, to understand the origin of the anti-influenza virus effect of WWMJ, I have investigated the flavonoids and metabolites by metabolome analysis. From analysis information, I conducted this study to comprehensively investigate the activity of major flavonoids against influenza A virus to construct a compound library, and to discuss the effects of different types and structures of flavonoids on the replication of influenza A virus.

In chapter II, I investigated the various compound in WWMJ using metabolome analysis. I also discussed the natural flavonoid activity against influenza A virus from the viewpoint of molecular structure.
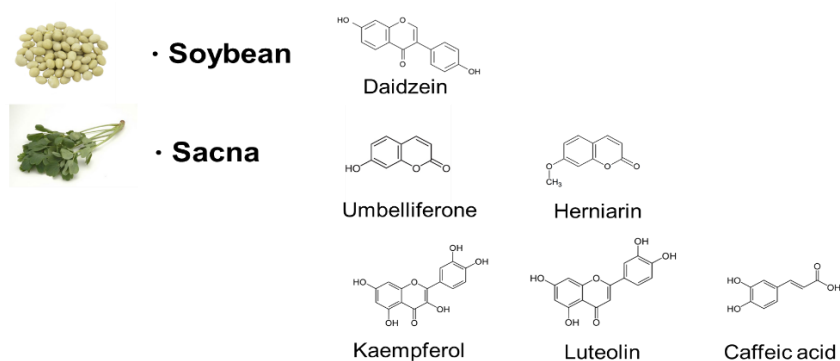
Figure 2-2. Anti-influenza virus effect of food components

The previous research [Reference 36, 37] shows food extract activity for influenza virus.

2.2. Materials and Methods

2.2.1. Metabolome analyses

The metabolomic data were obtained via LTQ O RBITRAP X L analysis (Thermo Fisher Scientific) using the Power Get software (http://www.kazusa.or.jp/komic s/ja/tool-ja/48-powerget.html) originally developed by the Kazusa DNA Research Institute [59]. Chromatographic separation was performed at 40°C using a TSK gel ODS-100V column (3 mm × 50 mm, 5 μm: TOSOH) on an Agilent 1200 series system. For separation, the mobile phases were optima grade water with 0.1% formic acid (A) and acetonitrile with 0.1% formic acid (B). A 25-min gradient at a flow rate of 0.4 ml/min with the following conditions was used: 0–5 min, held at 1% B; 5–10 min, linear gradient from 1% to 3% B; 10–18 min, linear gradient from 3% to 40% B; 18–22 min, linear gradient from 40% to 80% B; 22–27 min, column cleaning at 95% B; and 27–35 min, re-equilibration with solution A. The injection volume was 5 μl, and the MS was operated in the positive ion mode (ESI) with a scan range of m/z 100–1500 using one of the top five MS/MS methods. The average accurate mass of the compound peak was collated with a public database (Flavonoid Viewer) using Kazusa DNA Research Institute development Software (MF Searcher).

2.2.2. Compounds

Chrysin, luteolin, acacetin, biochanin A, naringenin, (−)-EGCG, (−)-EGC, (−)-EC, quercetin, myricetin, fisetin, and morin were purchased from Tokyo Chemical Industry Co., Ltd (Tokyo, Japan). Apigenin, daidzein, genistein, and kaempferol were purchased from Fujifilm Wako Pure Chemical Corporation (Osaka, Japan). Baicalein and hesperetin were purchased from Sigma-Aldrich Co. LLC (St. Louis, Missouri, USA). Tricetin,

eriodictyol, and isosakuranetin were purchased from Extrasynthese S.A. (Lyon, France). Pinocembrin was purchased from Toronto Research Chemicals, Inc (Toronto, Ontario, Canada). Galangin was purchased from ChromaDex (Los Angeles, Southern California, USA). All the compounds were dissolved in dimethyl sulfoxide, and samples were used within 3 months of preparation.

2.2.3. Cell and viruses

MDCK cells were grown in E-MEM containing 7% FBS (Lot No. S16984S1820, BioWest, Nuaillé, France). Type A influenza viruses H1N1 (PR/8/34, Osaka/2024/2009, Osaka/71/2011) were used in the experiments.

2.2.4. Determination of viral yield in the presence of samples

The effect of addition of flavonoid samples on viral yield was determined according to the procedure described previously [35].

2.2.5. Focus-reduction assay

FFRA was performed according to the method described previously [35]. I examined six concentrations of each flavonoid to generate data for the estimation of IC_{50} values.

2.2.6. Time-of-addition assay

I conducted a time-of-addition experiment as described previously [35]. DMEM containing flavonoids, which was approximately 1.4- to 4 times the median inhibitory concentration (IC_{50}), was added at – 1–0 h, 0–8 h, 0–4 h, and 4–8 h (replication). Furuta et al. [47] estimated the intracellular cycle of infected cells before extracellular budding

to be 8 h, and growth stages were assumed to occur at 4 h intervals.

2.2.7. Cell viability determination

Cell viability was determined using the Cell Proliferation Kit I (MTT) (F. Hoffmann–LaRoche Ltd, Basel, Switzerland). The CC_{50} values (representing the concentration of 50% cell viability as measured using the MTT assay) were determined. The cytopathic effect of virus-infected cells with various concentrations of flavonoids was observed with a microscope. This experiment was performed at a concentration that was not cytotoxic.

2.2.8. Statistical analyses

The amounts of virus determined in the time-of-addition assay and the antiviral assay were analyzed by the Student's t-test in Excel Toukei version 6.0 (Esumi). A p value of less than 0.05 was considered statistically significant.

2.3. Results and Discussion

2.3.1. Metabolomic data analysis of WWMJ

I conducted a metabolomic analysis to identify the active components in WWMJ, focusing on flavonoids that have been reported. Many low-molecular weight compounds were identified (1646), including 578 different flavonoids that comprised 35% of the total compounds present in the WWMJ (Table 2-1). There were 228 glycosylated flavonoids and 350 aglycons. Thus, the proportion of aglycons compared to all flavonoids detected was 61%. The WWMJ contained 173 prenylated flavonoids, which accounted for 30% of the detected flavonoids, and 172 of the prenylated flavonoids were aglycons. Some of the prenylated flavonoids detected are shown in Table 2-2. In the metabolome

analysis, 8-PN and 8-prenyldaidzein were detected in WWMJ, while daidzein, genistein, biochanin, kaempferol derivatives, secoisolariciresinol, pinoresinol, and glycosylated variants of the latter phytoestrogens were also present (data not shown). However, acacetin, kaempferol, resveratrol, glycitein, formononetin, coumestrol, 4-methoxycoumesterol, repensol, trifoliol, and lariciresinol were not detected.

Table 2-1. Classifying polyphenols in WWMJ based on backbone structure

Backbone name	Molecular weight	Numbers	%
Aurone, Chalcone	222, 208	83	14
Flavanone	224	99	17
Flavone	222	182	31
Dihydro flavonol	242	23	4
Flavonol	238	90	16
Flavan	210	6	1
Anthocyanin	207	0	0
Isoflavonoid	222, 210	91	16
Neo flavonoid	222, 210	4	1

Table 2-2. Classifying polyphenols based on ornamentation groups

| Glycosylation	Modification	Numbers
No	No	91
No	Alkylated	12
No	Prenylated	172
No	Possessing a furan group	22
No	Possessing a pyran group	53
O-glycoside	No	120
O-glycoside	Alkylated	1
O-glycoside	Prenylated	1
O-glycoside	Possessing a furan group	1
O-glycoside	Prenylpropanoid	8
C-glycoside	No	62
O- &C-glycoside	No	18
Others		17

2.3.2. Previous research and evaluation of flavonoids

In this chapter, I identified secondary metabolites, such as daidzein, genistein, biochanin, kaempferol derivatives, others. In previous study, Nagai and Kanazawa also identified such as daidzein, umbelliferone, herniarin, quercetin, luteolin, and caffeic acid, in food extracts [36, 37]. The IC_{50} values of these compounds against influenza A virus (PR/8/34) are 143.6 µM, 555.6 µM, 1306.8 µM, 274.8 µM, 8.0 µM, and 81.7 µM, respectively. In a previous study on the antiviral activity of two phenylpropanoids, umbelliferone and herniarin, the IC_{50} values were found to be 555.6 and 1306.8 µM, respectively. These data indicate that antiviral activity is affected by changes in the position of hydroxyl and methoxy groups in the basic skeleton. The activity may be related to electron transfer reactions and electron density differences based on the position of functional groups. These compounds of anti-influenza virus effects are generated as secondary metabolites in plants. To investigate the anti-influenza virus effects of these compounds, I focused on the major flavonoids. The activities of major flavonoid aglycons produced by plants are given in Figure 2-3 – Figure 2-7. It is calculated the IC_{50} values and evaluated the antiviral activity of the compounds using the SI value (CC_{50} / IC_{50}).

2.3.3. Flavone and isoflavone group

In the flavone group, six flavones with different modifying groups were prepared. The flavone skeleton showed strong antiviral activity compared with other classes, with IC_{50} values between 4.9 and 82.8 µM (Figure 2-3). The modification of the B ring from the 3′- to the 5′-position is important, and it is desirable that the hydroxyl group is on the 3′- and 4′- positions rather than on the 5′-position. Based on these findings, catechol structure may contribute to the anti-influenza virus activity. Furthermore, apigenin and luteolin

showed strong inhibitory effects ($IC_{50} \leq 10$ μM), and the SI also suggested that these are effective inhibitors. Nagai et al. [36] reported that daidzein demonstrated antiviral activity in MDCK cells, whereas genistein and biochanin A did not exhibit any activity (Figure 2-4). However, biochanin A is effective against A/H5N1 viral strains in A549 cells [60]; therefore, the mechanisms underlying the inhibition of virus growth could vary among different cell lines. The hydroxyl group at the 5-position of the A ring causes loss of the anti influenza effect in MDCK cells.
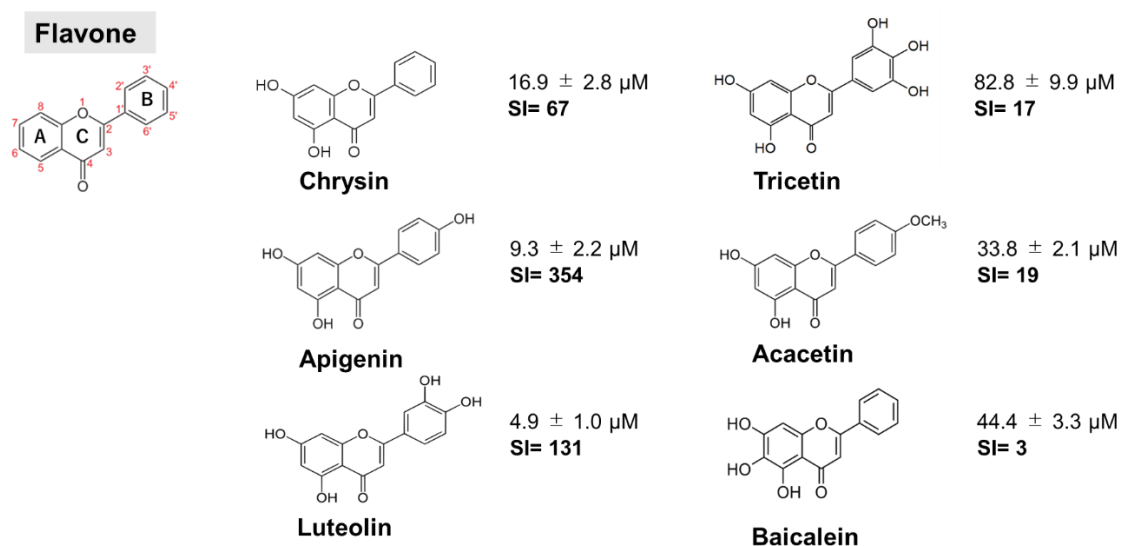
Figure 2-3. Anti-viral effect of flavone

Values are the average of the results obtained using various final concentrations of flavonoids and MDCK cells from three independent experiments. The IC_{50} of flavonoids is reported as μM. The values after " ± " in the IC_{50} are the standard deviations. The IC_{50} value of oseltamivir acid in the A/PR/8/34 strain was 2.0 ± 0.7 nM. Selectivity index = CC_{50}/IC_{50} (CC_{50}, 50% cytotoxicity concentration; IC_{50}, 50% half maximal inhibitory concentration). The SI value of oseltamivir was 622,222.
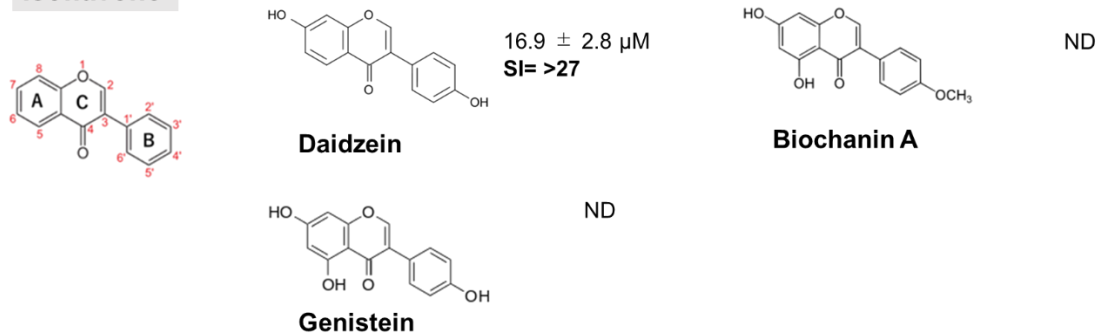
ND: not detected

Figure 2-4. Anti-viral effect of isoflavone

2.3.4. Flavonol group

Flavonols, commonly recognized as quercetin in onion, are effective against various viruses [61]. Here, I found that the IC_{50} values of the six evaluated flavonols was in the range from 62.9 to 477.8 μM (Figure 2-5). Flavonols were observed to have less antiviral activity than flavones, which may be due to the modified hydroxy group at the 3- position of C ring. Similar to isoflavones (genistein and biochanin A), the hydroxyl group at a specific position in the flavonoid backbone may reduce the anti-influenza virus activity. Based on the SI, the position of monohydroxy group on the B ring or the catechol structure is also important.
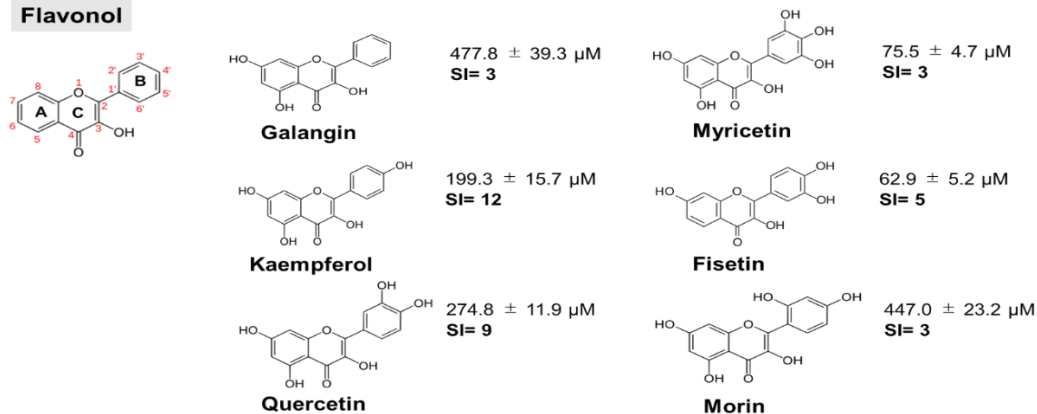

Figure 2-5. Anti-viral effect of flavonol

2.3.5. Flavanone

Zeng et al. [62] reported that naringenin, an aglycone flavanone, is a potential anti-inflammatory agent and an immunomodulator for various diseases. Therefore, the effect of aglycone flavanone on influenza virus should be examined for the development of a new therapeutic approach. In the present study, I investigated the activity of major flavanones, such as naringenin and hesperetin, and observed IC_{50} values of 290.4 to 881.1 µM (Figure 2-6). Compared with other classes of flavonoids, the anti-influenza virus activity of flavanones tended to decrease. In flavanones, the type of modifying group at the 3′- and 4′-positions of the B ring is directly involved in the antiviral activity, and a hydroxyl or methoxy group is preferable. Flavanone is saturated at the 2- and 3-positions of the C ring, and the B and C rings overlap to form a spherical structure. I considered that the steric factors of flavanone skeleton and modifying groups may determine the anti-influenza virus activity.
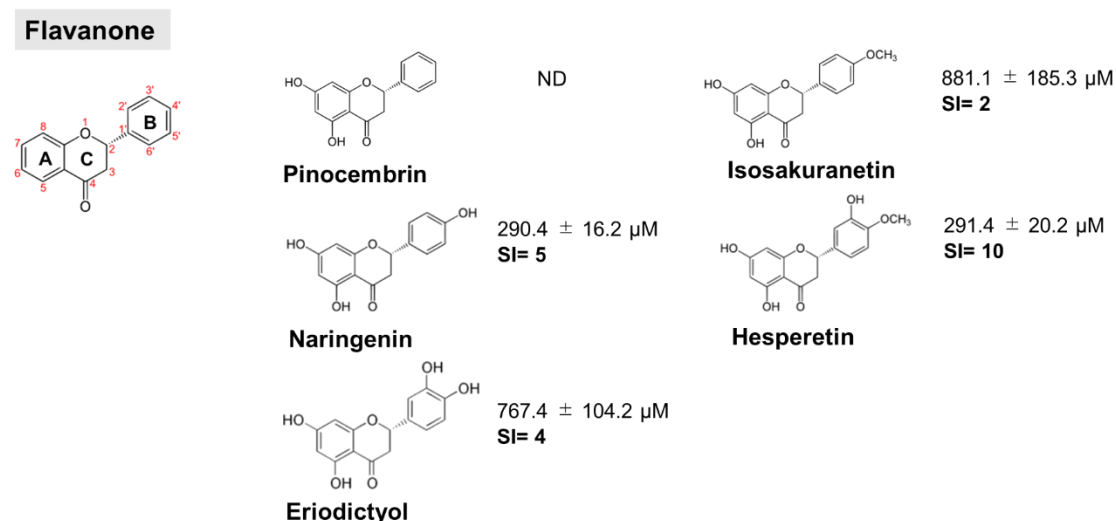

Figure 2-6. Anti-viral effect of flavanone

2.3.6. Flavan-3-ol

Xu et al. [34] reported the antiviral effects of catechins. Here, I used (-)-EC and its hydroxyl form (-)- EGC (Figure 2-7). EGC showed a strong antiviral effect, although its toxicity was increased. The results suggest that the anti-influenza virus effects might significantly depend on the stereoisomer of catechin and the modifying groups present. The cytotoxicity of flavonoids was determined using an MTT assay kit. The results suggest that the flavonoid structure is one of the factors that determine cell toxicity (Figure 2-8). Thus, these compounds may have anti-influenza virus activities, but their clinical application is limited owing to the cytotoxic effects. Baicalin, myricetin, fisetin, and EGC include pyrogallol or similar structures in their molecules (Figure 2-8.D), which may affect mitochondria and cause cytotoxicity when intracellular concentrations exceed certain levels.
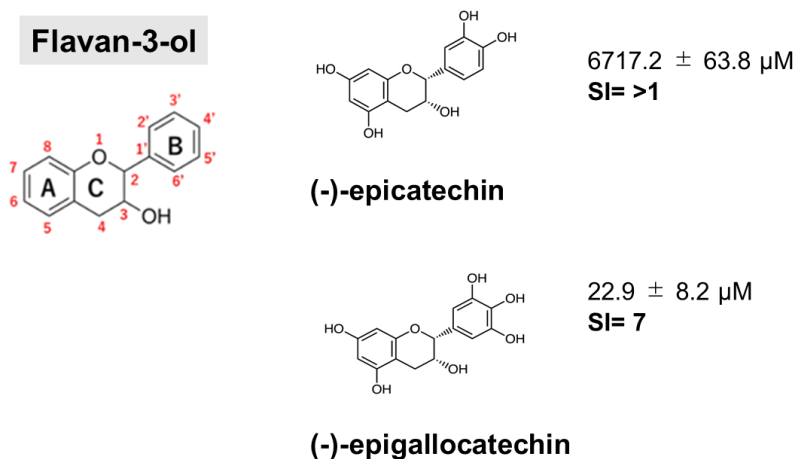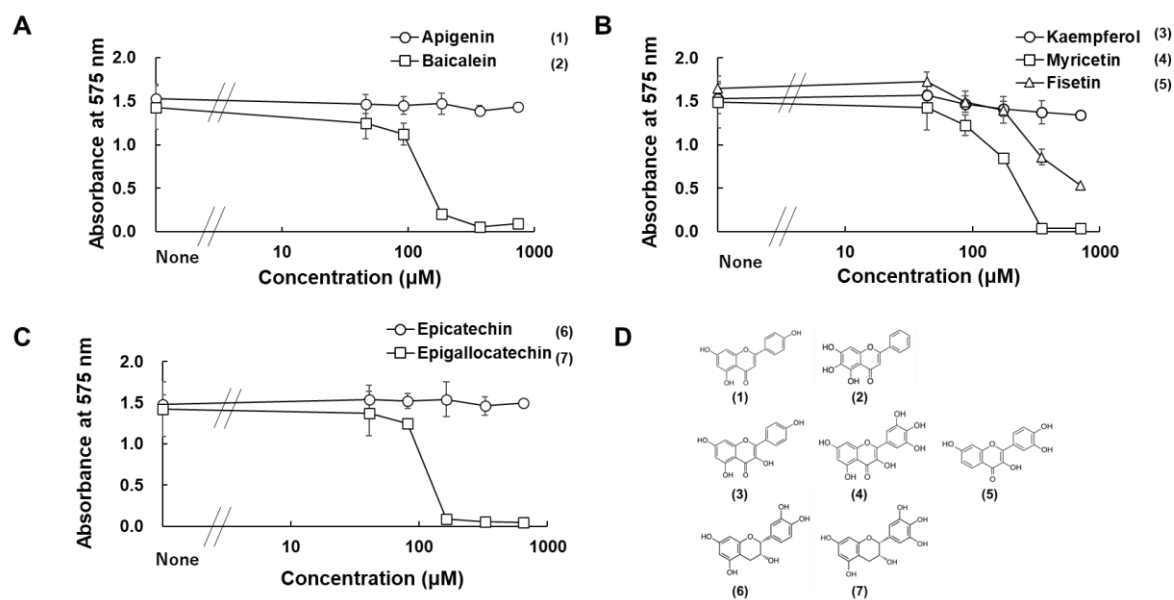

Flavan-3-ol

6717.2 ± 63.8 μM
SI= >1

(-)-epicatechin

22.9 ± 8.2 μM
SI= 7

(-)-epigallocatechin

Figure 2-7. Anti-viral effect of flavan-3-ol

**Figure 2-8. The cytotoxicity of different flavonoids and their structures.**

A (1) Apigenin and (2) Baicalein, **B** (3) Kaempferol, (4) Myricetin, (5) Fisetin, **C** (6) (–)-Epicatechin, and (7) (−)-Epigallocatechin (EGC). Cytotoxicity was determined using the MTT assay. MDCK cells were treated with the flavonoids at different concentrations (μM) for 24 h. Cytotoxicity measurements were performed as described in the assay manual. Data are representative of three independent experiments. Bars on each point represent the standard deviation. **D** Structures of flavonoids (1) – (7).

Among the 22 compounds investigated in this study, 19 flavonoids inhibited the replication of type A influenza virus.

2.3.7. Time-of-addition assay

To investigate the mechanism of virus inhibition by major flavonoids, such as apigenin, daidzein, kaempferol, naringenin, and EGC, I performed a time-of-addition assay (Figure 2-9). A characteristic inhibition was confirmed in each flavonoid class. Apigenin, daidzein, and EGC did not inhibit virus adsorption (−1–0 h) (Figure 2-9. A, B, E). Conversely, naringenin and kaempferol inhibited not only the replication of the virus but also its adsorption. Compared with each control, kaempferol (315 μM) and naringenin (478 μM) inhibited viral adsorption by approximately 54% (Figure 2-9.C) and 42%

(Figure 2-9.D), respectively. Hanada et al. [63] reported that 8-prenylnaringenin strongly inhibited the virus adsorption; these results suggested that the modifying groups of flavonoids contribute to the viral adsorption phase including endocytosis. All flavonoids except daidzein decreased the viral growth in the early stage of viral infection (0–4 h). Kaempferol and naringenin also showed low inhibitory effects in the early stage (0–4 h). Other flavonoids also inhibit the early stage of influenza virus infection [64, 65], and they can be potentially used for controlling the infection. Additionally, flavonoids commonly inhibit the late stage (4–8 h) of viral replication [63, 66-68], suggesting that they may regulate intracellular immunity or late viral replication events before the release of viral particles.

39
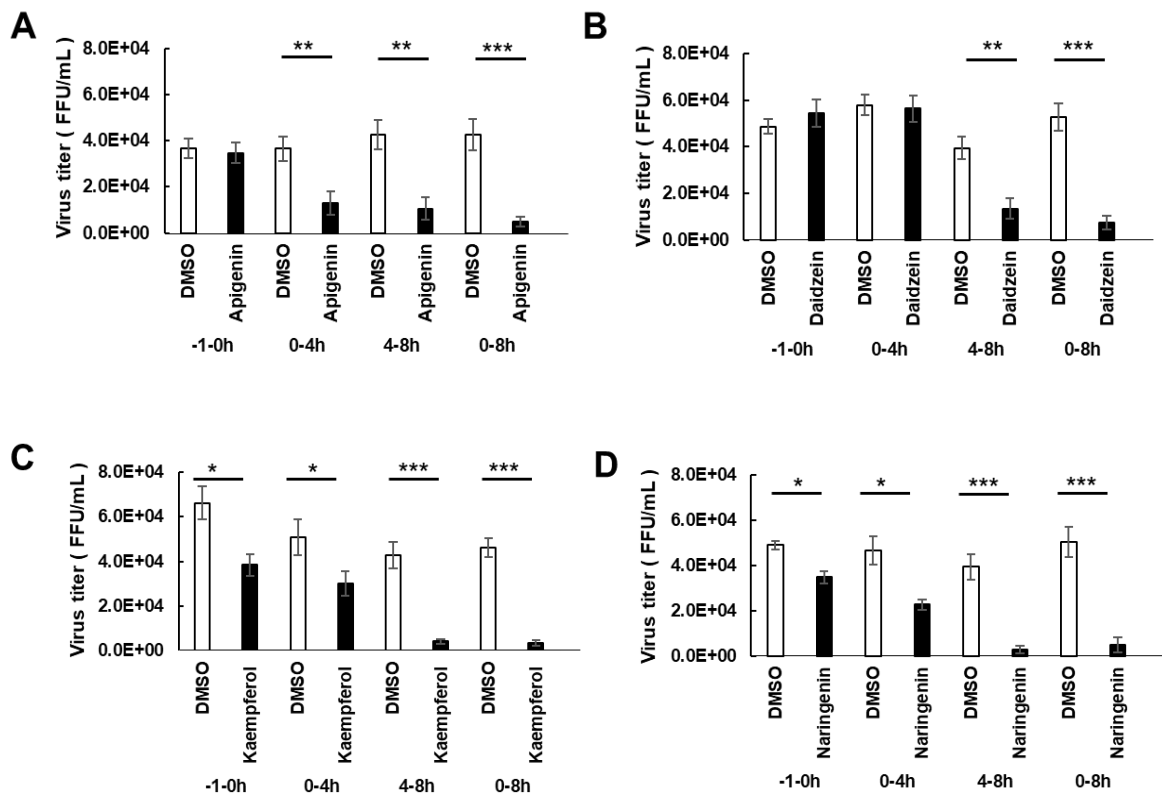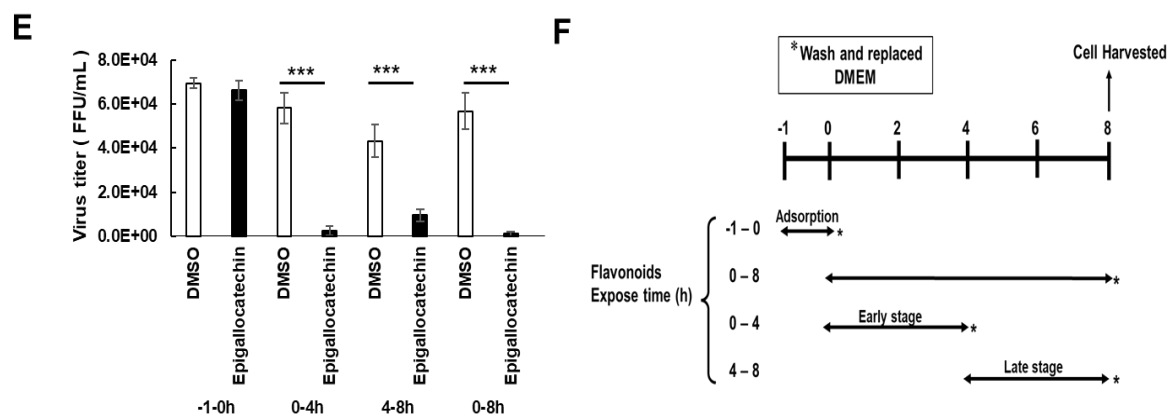
Figure 2-9. The inhibition stages of the flavonoids in virus multiplication and experiment schedule.

The inhibition stages of flavonoids in virus multiplication and the experimental schedule. **A** Flavone (Apigenin, 37 μM), **B** isoflavone (Daidzein, 236 μM), **C** flavonol (Kaempferol, 315 μM), **D** flavanone (Naringenin, 478 μM), **E** flavan-3-ol (Epigallocatechin, 33 μM), and **F** experiment schedule (flavonoids in DMEM were added at the times and periods shown). MDCK cells were infected with influenza virus A/PR/8/34 at a multiplicity of infection of 0.01 in 24-well plates. After infection at each time point, the cells were harvested and viruses were assayed using the focus-forming reduction assay. White columns, mean viral yields of control cells; black columns, mean viral yields of cells treated with each flavonoid. Data are representative of three independent experiments. The standard deviation bars are indicated on each bar graph. ***$p < 0.001$, **$p < 0.01$, *$p < 0.05$
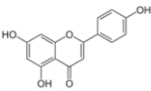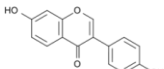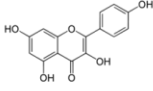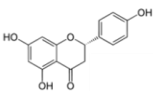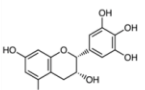
To further investigate the mechanism of inhibition by flavonoids, I evaluated their activities against oseltamivir-resistant strains (Osaka/2024/2009 and Osaka/71/2011). All flavonoids, except daidzein and EGC, inhibited the growth of these two strains. Daidzein showed no inhibitory effect on the Osaka 2024/2009 strain, whereas EGC was not effective against the resistant strains. As some flavonoids were also effective against the resistant strains (Table 2-3), a mechanism of action different from that of oseltamivir during the late growth phase (4–8 h) of influenza A virus might be operative. Although it has been suggested that flavonoids bind to the active site of NA and attenuate its enzymatic activity [69], further studies confirming the mechanisms of virus inhibition by

40

flavonoids are needed. Because EGC showed no detectable inhibitory effects on the resistant strain, it may inhibit viral growth via a mechanism similar to that of oseltamivir. The IC_{50} and SI values suggested that apigenin might be effective against various type A strains, including the oseltamivir-resistant strains. In contrast to existing antiviral drugs that target specific viral growth processes, flavonoids have multiple modes of inhibition, which may be an advantage in dealing with the emergence of antigen-mutated viruses. Lipophilic compounds, such as aglycons, exert their effects by binding to cytoplasmic or nuclear receptors [70]. Kanazawa et al. [71] reported the intracellular uptake of major flavonoids, such as apigenin. To investigate the inhibitory mechanism during the -1–0 h (adsorption) and 0–4 h (early stage) stages of infection, it is necessary to measure the concentration of each flavonoid and related metabolites taken up by MDCK cells. Flavonoids and viruses are "foreign bodies," and they contribute to the activity of the natural biological defense system. Recently, Kesic et al. [72] proposed that inhibition of the transcription factor, AhR, which supports the metabolism of foreign bodies, and activation of the Nrf2, can improve the symptoms of influenza virus. Nrf2 plays an important role in redox regulation during influenza virus infection [73]. (-)-EGCG exhibits antiviral activity that involves antioxidation [74], suggesting that flavonoids modulate the intracellular redox state.

Table 2-3. Anti-viral effects of flavonoids against oseltamivir resistant strain

[a] Values are the average of the results obtained using various final concentration of flavonoids and MDCK cells from three independent experiments. The IC_{50} of flavonoids is reported as μM. The top row shows the IC_{50} value in the Osaka2024/2009 strain and the bottom row shows the IC_{50} value in the Osaka71/2011 strain. The values after "±" in the "IC_{50} value" column are the standard deviations. The IC_{50} values of oseltamivir acid in the resistant strains (Osaka2024/2009 and Osaka71/2011 strain) were 577±19 nM and 865±17 nM, respectively. [b] Selectivity index = CC_{50}/IC_{50} (CC_{50}, 50% cytotoxicity concentration; IC_{50}, 50% maximal inhibitory concentration). The SI values of oseltamivir were 1,556 and 1,037, respectively.

ND: Not Detected

Class	Compound name and structure		IC_{50} value [a] (μM)	SI [b]
Flavone	Apigenin		23.3 ± 7.4 76.7 ± 7.8	40 12
Isoflavone	Daidzein		ND 186.2 ± 5.9	ND >21
Flavonol	Kaempferol		158.4 ± 8.0 175.9 ± 14.7	6 5
Flavanone	Naringenin		321.0 ± 69.5 466.9 ± 36.8	4 3
Flavan-3-ol	(-)-Epigallocatechin		ND ND	ND ND

As plant-derived secondary metabolites, flavonoids are also involved in the host immune response systems. Immune response and *in vivo* oxidation are closely related, and cellular oxidative stress is induced by daidzein [54]. Further studies on lipid oxidation signals linked to the anti-influenza virus effect of isoflavones are required. Several mechanisms underlying the effects of flavonoids have been explained, it is involved in the intracellular redox reaction, at least in part, and in the immunomodulatory function of the host cells. Furthermore, flavonoids have been reported to carry metal ions to cells as ionophores [75], which can contribute to anti-influenza virus effects [76], and thereby, advance the development of new approaches.

Chapter III

Effect of structural differences in naringenin, prenylated naringenin, and their derivatives on the anti-influenza virus activity and cellular uptake of their flavanones

3.1. Introduction

The influenza virus is an RNA virus that belongs to the family *Orthomyxoviridae*, which mainly causes infections in mammals. While the spread of COVID-19 appears to have reduced influenza virus infections [77], co-infections in animals [78] and humans [79] have been reported. Influenza virus has caused pandemics, with many reported deaths [80, 81]. Due to its susceptibility to antigenic variation [82], influenza virus may cause a pandemic in the future.

Several agents have been developed for the treatment of influenza. M2 channel blockers (amantadine and rimantadine), neuraminidase inhibitors (oseltamivir, zanamivir, peramivir, and laninamivir), viral RNA polymerase inhibitors (favipiravir), and cap-dependent endonuclease inhibitor (baloxavir marboxil) are known. Antiviral drugs, such as oseltamivir, act directly on the virus multiplication mechanism. However, successive reports of drug-resistant strains or potential have been reported [83, 84]. Lampejo [85] warned that new antiviral strategies should be considered when preparing for a pandemic. Natural plant compounds are important sources for future drug development. Flavonoids are plant secondary metabolites classified as polyphenols. Naringenin is classified as a flavanone and is present in plants such as citrus fruits and others [86–88]. Flavanone group compounds and derivatives have broad-spectrum biological activity [89–94] and

have attracted attention as antiviral agents [95]. Recently, the physiological functions, including biological and pharmacological effects of prenylated compounds have been reported [96–100]. Hanada previously reported that 8-prenylnaringenin (8-PN) isolated from wild watermelon (*Citrullus lanatus* var. *citroides*) exhibits high antiviral activity [63]. Therefore, I believe that plants rich in prenylated compounds have the potential to be important sources for antiviral drug development strategies. For example, xanthohumol, 8-PN, and 6-prenylnaringenin (6-PN), which are produced by hop (*Humulus lupulus* L.) [101, 102].

Additionally, I have reported that the antiviral activity of flavonoids depends on the type and structure of the modifying group, suggesting that this may be due to the differences in substituent position, steric effect, and coordination effect of the compound [103]. When considering anti-influenza virus strategies, it is important to study the effects of these chemical structures and the pharmacokinetics of tissues and cells. Mukai et al. [104] reported the cellular uptake of flavonols, quercetin, and 8-prenyl quercetin. However, the cellular distribution of prenylated naringenin has not been fully investigated. Therefore, in this chapter, to investigate the chemical and pharmacological properties related to antiviral activity, derivatives with several substituents with different properties were synthesized to elucidate the relationship between the cellular uptake and intracellular distribution of prenylated naringenin and its antiviral activity.

3.2. Materials and Methods

3.2.1. Compounds

To investigate the viral effects of chemical structure, synthesized compounds based on 8-PN and 6-PN. The chemical structures of the compounds were confirmed using ^{1}H NMR

(500 MHz) and ^{13}C NMR (125 MHz). The synthesized compound information and materials method showed https://doi.org/10.3390/ph15121480.

3.2.2. Cell and viruses

MDCK cells were grown in E-MEM containing 7% FBS. Type A influenza virus H1N1 (PR/8/34) was used in the experiments. To infect the cells, the virus was diluted in serum-free MEM containing 0.04% BSA (fraction V; Sigma-Aldrich) and incubated with the cells at a multiplicity of infection of 0.001 for 1 h at 37 °C. The medium was then removed and replaced with serum-free DMEM containing 0.4% BSA and 2 µg/ml acetyl trypsin (Sigma-Aldrich) for the remainder of the infection period. For fluorescence microscopy, cells were grown in DMEM (Wako) without phenol red containing 1% FBS and 2 mM glutamine.

3.2.3. Cell viability determination

Cell viability was determined using the Cell Proliferation Kit I (MTT) (F. Hoffmann–La Roche Ltd., Basel, Switzerland). The cytopathic effect on the virus-infected cells treated with various concentrations of flavonoids was observed under a microscope. The experiment was performed at a concentration that was not cytotoxic.

3.2.4. Determination of cell viability in the presence of naringenin derivatives

The effects of naringenin derivatives on viral yield were determined according to a previously described procedure [35, 105]. The focus-forming reduction assay for viral activity was performed according to a previously described procedure [35, 105].

3.2.5. Cellular uptake of naringenin and its derivatives

Fluorescence microscopy experiments were performed according to Wolff et al. [106].

Briefly, cells were plated in glass-bottom dishes (Matsunami, Osaka, Japan) and cultured in a medium without phenol red. Cells were exposed to 30 μM naringenin and its derivatives, and phase-contrast and fluorescence images were acquired for a fixed exposure time before and after the addition of the compounds at defined intervals. For the imaging, I prepared a custom-built filter (excitation 470/40, emission 605/70). Upon excitation at approximately 470 nm (bandwidth of 40 nm), a major emission was observed at approximately 605 nm (bandwidth of 70 nm). The emission signal from naringenin and its derivatives was detectable at wavelengths >565 nm, making it possible to design filters that avoid cellular autofluorescence in the green range.

Fluorescence microscopy of living and fixed cells was performed using an inverted fluorescence phase-contrast microscope (Keyence BZ-X800), consisting of an infinity optical system (Nikon CFI60 series with software BZ-H4 series; Keyence, Osaka, Japan).

3.2.6. Estimation of intracellular naringenin and prenylated naringenin

Cells were cultured on glass plates and incubated in a medium supplemented with the compound for 180 min. They were then washed and fixed with 4% paraformaldehyde for 30 min. After washing with PBS, DAPI staining was performed. Intracellular distribution was photographed and observed using an inverted fluorescence phase-contrast microscope (Keyence BZ-X800).

3.2.7. Time-of-addition assay

I conducted a time-of-addition assay as previously described [35, 105]. DMEM

containing prenylated naringenin (30 μM) was added at -1–0 h (adsorption), 0–8 h (replication), 0–4 h, 0–2 h, 2–4 h, 4–8 h, 4–6 h, and 6–8 h. Furuta et al. [47] estimated the intracellular cycle of infected cells before extracellular budding to be 8 h, and growth stages were assumed to occur at 2 h intervals.

3.2.8 Statistical analyses

The amounts of virus determined in the time-of-addition assay and the antiviral assay were analyzed by the Student's t-test in Excel Toukei version 6.0 (Esumi). Values are presented as means ± standard deviations (SD). A p-value $p < 0.05$ was considered statistically significant.
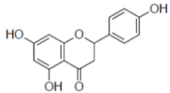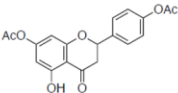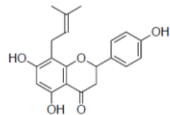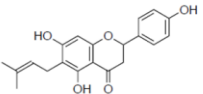
3.3. Results

3.3.1. Anti-influenza activity of prenylated naringenin (8-PN, 6-PN) and other derivatives (1a–2d)

First, I have evaluated four compounds (naringenin, naringenin-4',7'-diacetate, 8-PN, and 6-PN). The IC_{50} value of naringenin was 290 μM. Additionally, naringen-in-4',7'-diacetate markedly lost its anti-influenza activity. Prenylated naringenin, 8-PN and 6-PN, showed strong activity with IC_{50} values of 24 and 38 μM, respectively (Table 3-1). Compared to naringenin, prenylation of the 8- or 6-position dramatically increases anti-influenza virus activity. However, no significant difference in activity was observed between the 8- and 6-position substituents. The other derivatives showed IC_{50} values in the range of 42 to 103 μM (Table 3-2, -3).

Table 3-1. Anti-viral effects of prenylated naringenin and derivatives.

[a]Values are the average of the results obtained using various final concentration of compounds and MDCK cells from three independent experiments. The IC_{50} of compounds were reported as μM. The values after "±" in the IC_{50} are the standard deviations. The IC_{50} value for oseltamivir acid in the A/PR/8/34 strain was 2.0 ± 0.7 nM. [b] Selectivity index=CC_{50}/IC_{50}(CC_{50}, 50% cytotoxicity concentration; IC_{50}, 50% maximal inhibitory concentration)
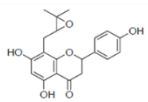
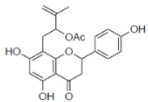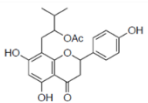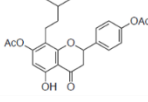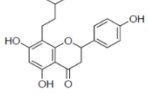ND: Not detected.

Compound name	structure	IC_{50} value [a] (μM)	SI [b]
(±)- Naringenin (Na)		290.4 ± 16.2	4.9
Naringenin-4',7'-diacetate (Na-di)		ND	ND
8-prenylnaringenin (8-PN)		24 ± 0.6	4.9
6-prenylnaringenin(6-PN)		38 ± 4.7	5.5

3.3.2. Coordination effect of modifying groups on the naringenin skeleton 8-position

Next, I have evaluated the effect of unshared electron pairs **1a**, **1b**, and **1e**. Compound **1a**, in which an epoxide group was introduced into the molecular structure, showed activity at 59 μM, but was less active than 8-PN. The activities of **1b** and **1e** were lost. In addition, to evaluate the coordination ability of the double bonds in the molecular structure at the 8-position, additional compounds were synthesized. The IC_{50} values of compounds **1c** and **1d**, which are saturated hydrocarbon side chains, were 42 and 61 μM, respectively (Table 3-2).
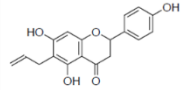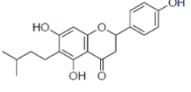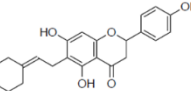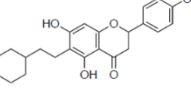
Table 3-2. Anti-viral effects of 8-position derivatives.

Compound name	structure	IC$_{50}$ value [a] (μM)	SI [b]
1a		59 ± 9.0	2.7
1b		ND	ND
1e		ND	ND
1c		42 ± 2.1	6.3
1d		61 ± 14.0	3.0

3.3.3. Stereoscopic effect of modifying groups on the naringenin skeleton

Previous studies have also suggested the effect of steric factors on the anti-influenza virus effect [103]. Subsequently, to investigate the steric effect, substituents with different steric effects (allyl groups: **2a**, isopentyl group: **2b**, cycloalkanes: **2c** and **2d**) were introduced. Compounds **2a** and **2b** showed weaker activities than 6-PN. The activities of **2c** and **2d** were not detected. In addition, isopentyl derivatives (**1d** and **2b**), showed lower activity than prenylated naringenins (Table 3-3).

Table 3-3. Anti-viral effects of 6-position derivatives.

Compound name	structure	IC_{50} value [a] (µM)	SI [b]
2a		103 ± 3.8	0.8
2b		58 ± 15.2	1.3
2c		ND	ND
2d		ND	ND

3.3.4. Uptake of naringenin and prenylated naringenin into Madin–Darby canine kidney (MDCK) cells

From the obtained results, it was found that the substituents in the flavanone skeleton greatly affected antiviral activity. To confirm the relationship between compound uptake and antiviral activity, I have evaluated intracellular uptake by fluorescence microscopy. The experiment was conducted by modifying the method described by Wolf et al. [106]. Figure 3-1, 2, 3 summarize the fluorescence intensity of each compound per 20 cells at each time point. This fluorescence intensity transition was also confirmed by the images. Images obtained after 180 min are shown in Figures 3-1-B, 2-B, and 3-B. Several compounds increased the fluorescence intensity after 120 min, reaching plateaus between 180 and 360 min. Naringenin, naringenin-4',7'-diacetate, 8-position derivatives, and 6-position derivatives showed low fluorescence intensity, whereas 8-PN and 6-PN showed high fluorescence intensity (Figure 3-1-A, 3-2-A, and 3-3-A). This fluorescence intensity

transition was also confirmed by the images (Figure 3-1-B, 3-2-B, and 3-3-B). In addition, the isopentyl group (**1d**) showed stronger fluorescence intensity than the other compounds. The fluorescence intensity at 360 min decreased in the order of 8-PN > 6-PN > **1d** > other compounds.
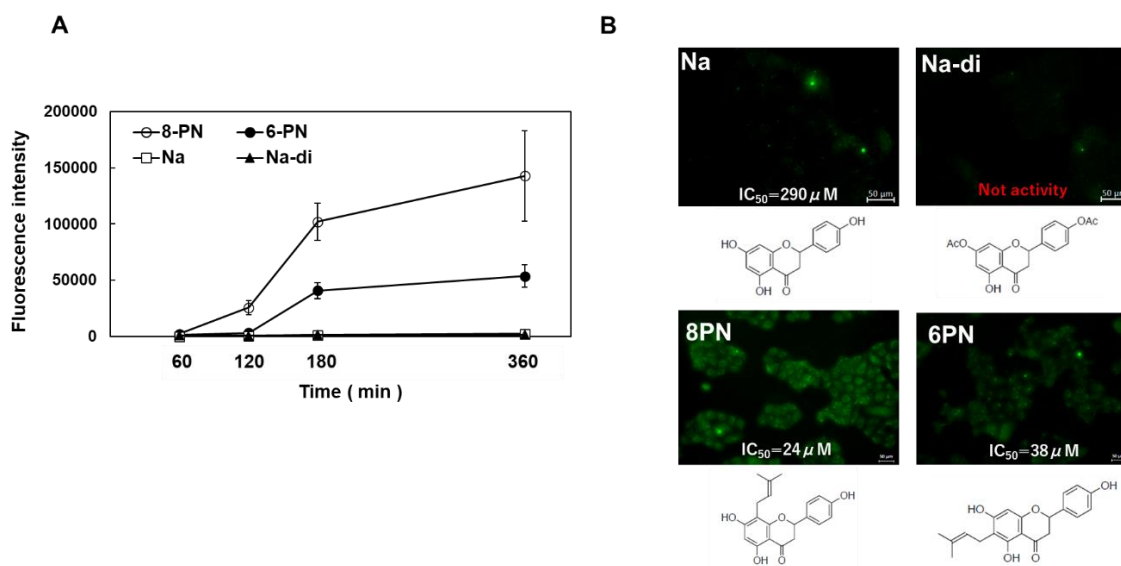
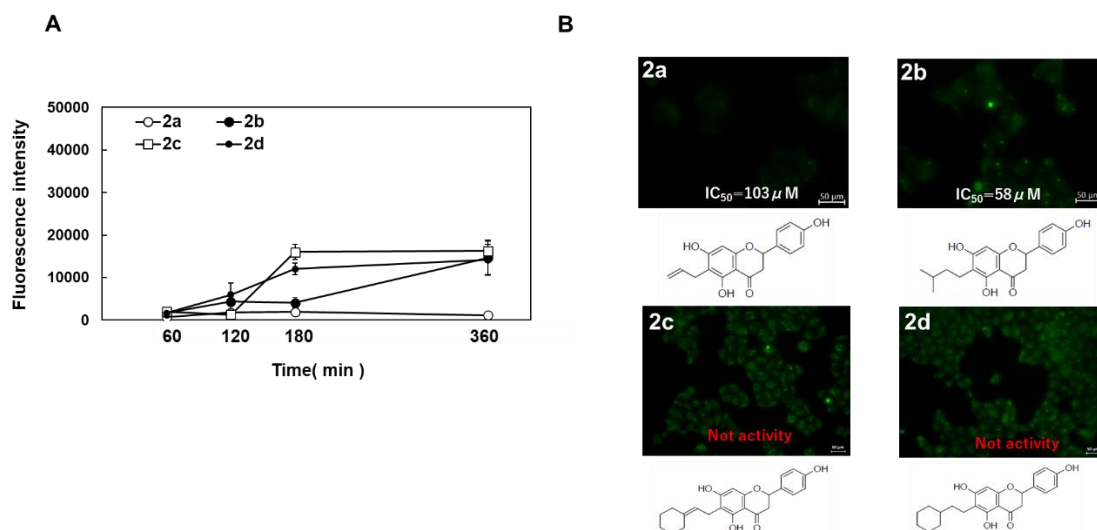**Figure 3-1. Time course and fluorescence images of prenylated naringenin and other derivatives.** (**A**) Fluorescence intensity of 8-PN, 6-PN, naringenin, and naringenin-4',7'-diacetate. (**B**) Fluorescence images.
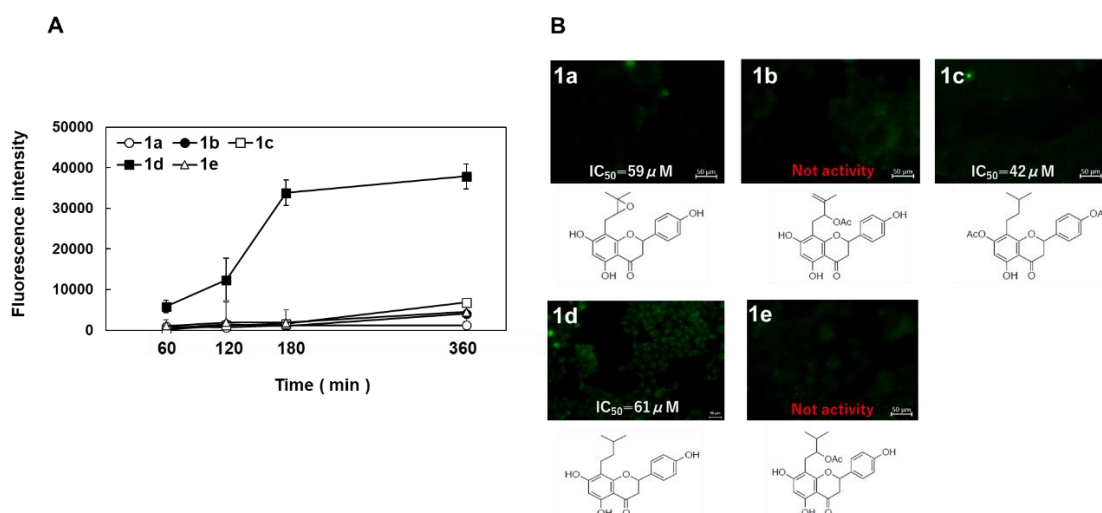
Figure 3-2. Time course and fluorescence images of 8-position naringenin derivatives.
(**A**) Fluorescence in-tensity of 8-position naringenin derivatives. (**B**) Fluorescence images

Figure 3-3. Time course and fluorescence images of 6-position naringenin derivatives.

(**A**) Fluorescence in-tensity of 6-position naringenin derivatives. (**B**) Fluorescence images. Madin–Darby canine kidney (MDCK) cells were treated with 30 μM of the compound in phenol red-free medium. We measured the mean fluorescence intensity at each time point (60, 120, 180, and 360 min), which was calculated from approximately 20 cells per time point. (**B**) Images show cells after 180 min of compound treatment. Scale bars = 50 μm

3.3.5. Intracellular distribution of naringenin and prenylated naringenin

Based on these results, I investigated the intracellular distributions of naringenin and prenylated naringenin. Cells cultured on glass plates were exposed to a concentration of 30 μM for 180 min. The exposed cells were washed with PBS and the compounds were removed from the medium. The cells were then fixed with 4% paraformaldehyde and observed under a fluorescence microscope. At 30 μM, the intracellular prenylated naringenin group showed a remarkable fluorescence pattern (Figure 3-4). The amount of naringenin taken up by the cells may be small. Moreover, fluorescence was detected for prenylated naringenin. I confirmed that 8-PN was distributed mostly in the cytoplasm and nucleus, while 6-PN tended to localize to the cytoplasmic periphery.
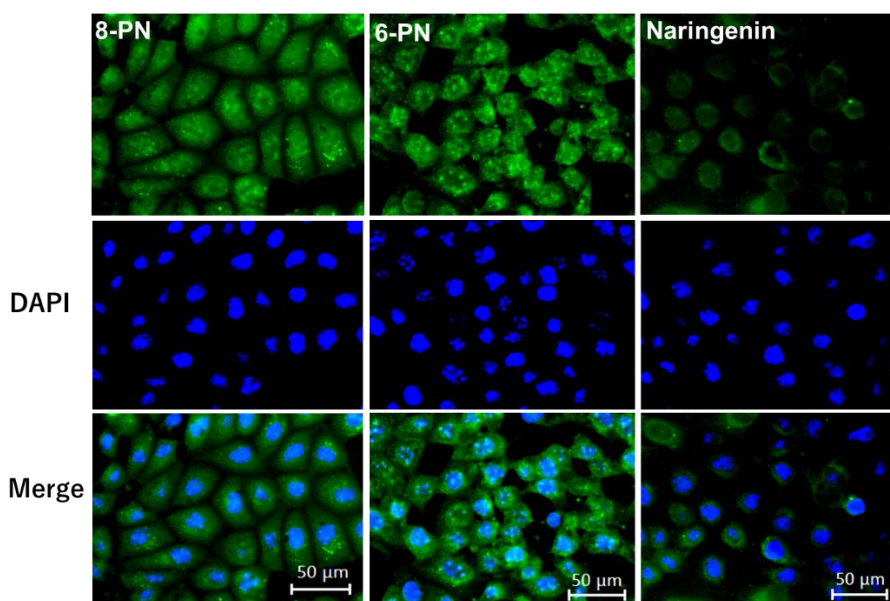
Figure 3-4. Analysis of prenylated naringenin and naringenin fluorescence distribution by imaging. After removing the medium, cells were treated with 30 μM compound for 180 min and fixed with 4% paraformaldehyde. Fixed cells were stained with DAPI (blue). These images show fluorescence of 8-prenylnaringenin (8-PN; left), 6-prenylnaringenin (6-PN; center), and naringenin (right). Scale bars = 50 μm.

3.3.6. Extracellular kinetics of prenylated naringenin

Based on our results, I have examined the kinetics of intracellular prenylated naringenin in DMEM containing 1% FBS. After 180 min of exposure, the cells were cultured in compound-free medium and fluorescence was observed at each time point. Consequently, each prenylated naringenin exhibited different kinetics. Intracellular 8-PN was released from the cell slowly, while 6-PN was released relatively quickly (Figure 3-5 and 3-6). The intracellular kinetics changed greatly depending on the position of the prenyl group. After 120 min of culturing in the medium, the fluorescence intensity of 8-PN and 6-PN increased approximately 1.6-fold and 9.4-fold, respectively, compared to that at 0 min (Figure 3-6).
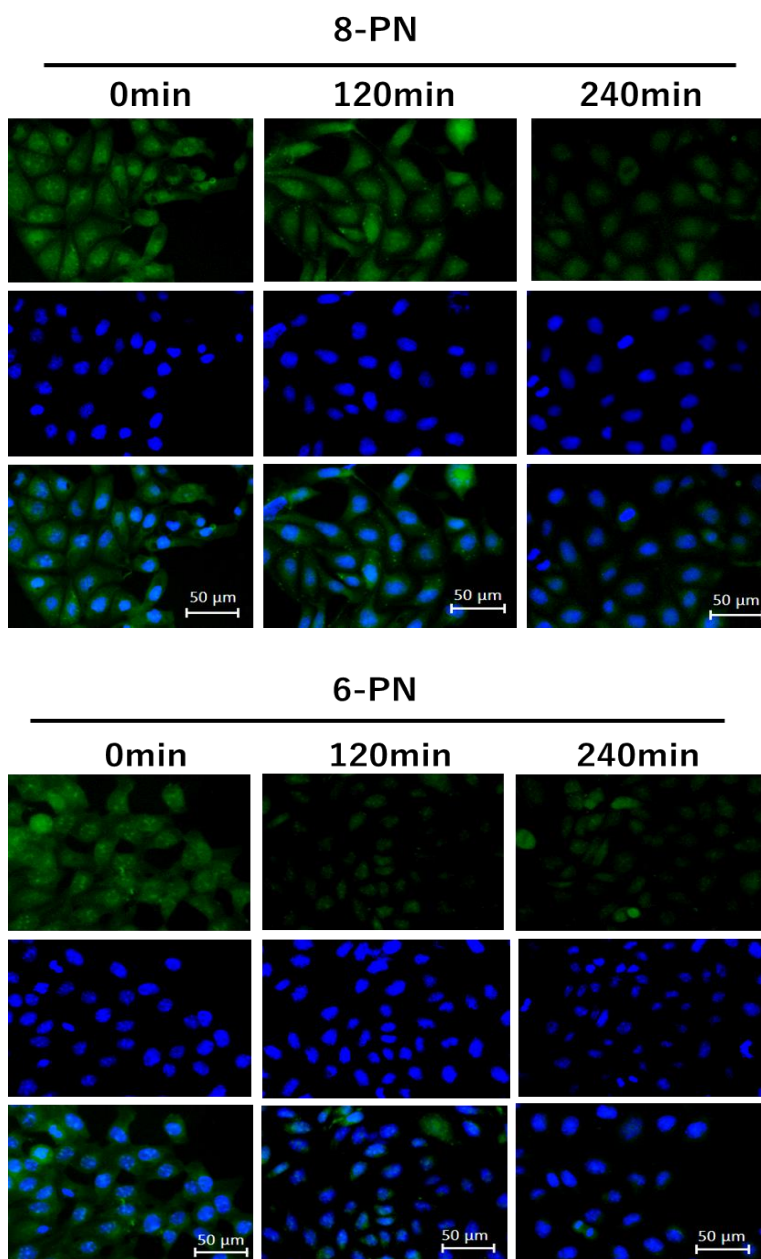
Figure 3-5. Efflux of prenylated naringenin after intracellular saturation. The amount of the compound in the cells was saturated by exposure for 180 min, and the cells were cultured in Dulbecco's Modified Eagle Medium (DMEM) for 0, 120, and 240 min. After removing the medium, cells were fixed with 4% paraformaldehyde and stained with DAPI (blue). These images show 8-PN and 6-PN fluorescence. Scale bars = 50 μm
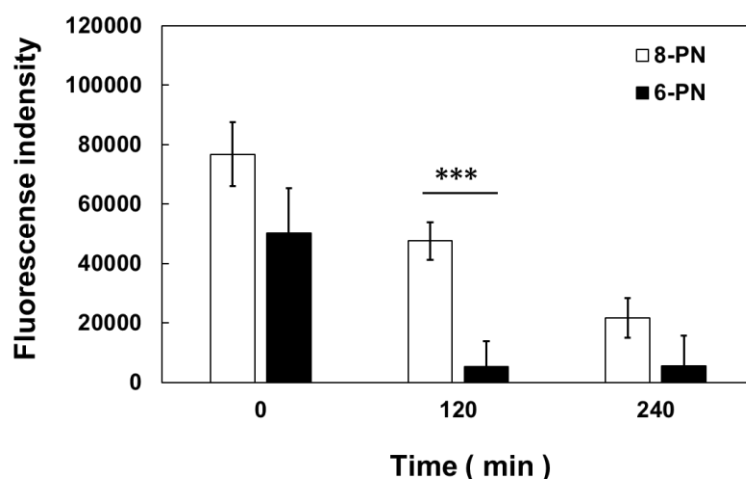
Figure 3-6. Efflux and fluorescence intensity of intracellular prenylated naringenins.
Fluorescence intensity of 8-PN and 6-PN from Figure 3-5 (120min). The standard deviation bars are indicated on each bar graph. ***$p < 0.001$.

3.3.7. Growth of influenza virus was inhibited by prenylated naringenin

I performed a time-of-addition assay to verify the effect of the prenyl group position on viral growth inhibition. Figure 3-7-A and 3-7-B show virus viability when exposed to each prenylated naringenin for each time duration. It was commonly inhibited after infection at the late stage (4–8 h, 6–8 h). However, 8-PN and 6-PN showed characteristic inhibition, depending on the position of the prenyl group. When exposed to prenylated naringenin during the virus adsorption period (-1–0 h), 8-PN was confirmed to have a high inhibitory effect. Conversely, 6-PN showed a high inhibition tendency during a 2-hour exposure time (4–6 h). In previous studies, inhibitory effects differed depending on the flavonoid back-bone [103]. The anti-influenza virus effect depends on the position of the prenyl group, which is a novel observation of the present study.
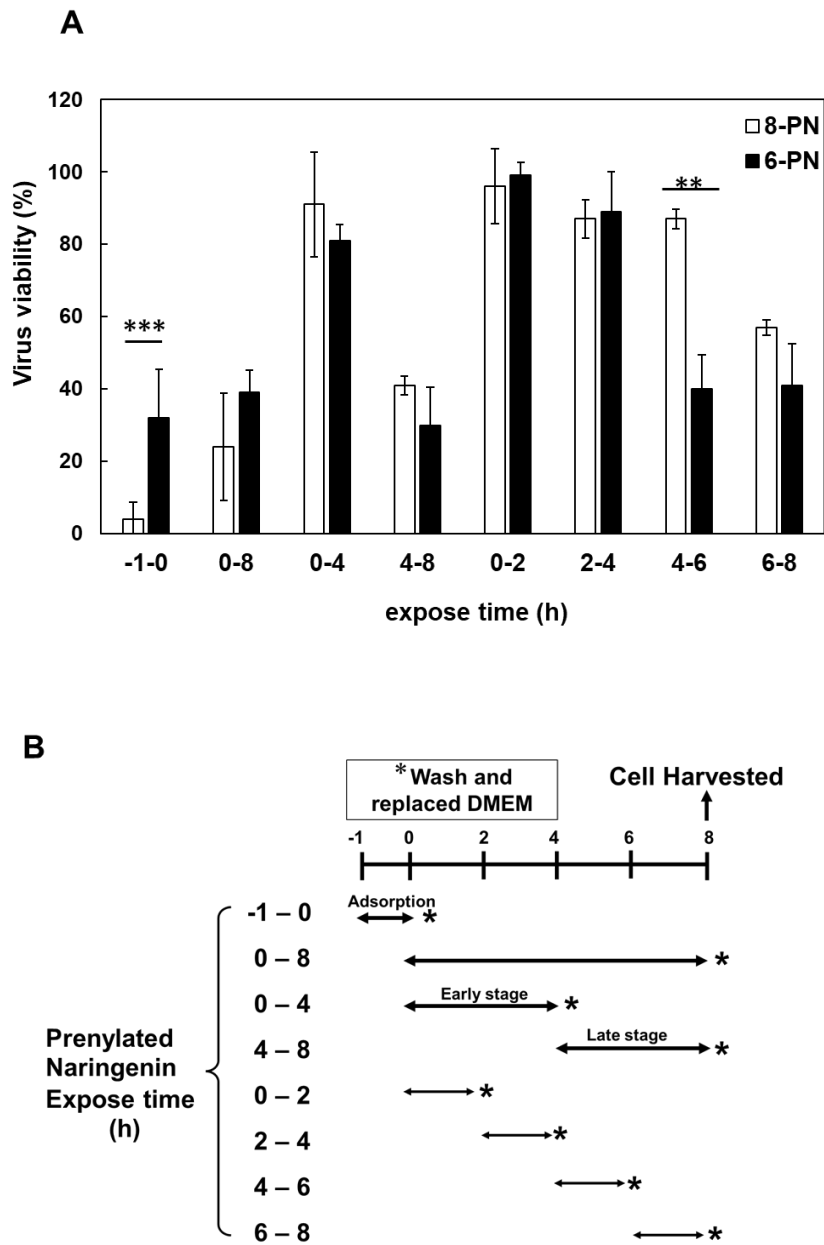
Figure 3-7. Effect of prenylated naringenin on virus viability. (**A**) 8-PN and 6-PN (30 μM). (**B**) Schedule of the experiment. Cells were infected with influenza virus A/PR/8/34 at a multiplicity of infection of 0.01 in 24-well plates. After infection at each time point, the cells were harvested and viruses were assayed using a focus-forming reduction assay. Each column shows virus viability at each stage of virus growth induced by 8-PN and 6-PN. Data are representative of three independent experiments. Standard deviation bars indicate each bar graph (***$p < 0.001$, **$p < 0.01$).

3.4. Discussion

The antiviral effects of some flavonoid aglycones and their derivatives have been investigated [107, 108] and have the potential to inhibit each viral growth stage [69, 75, 109]. Naringenin has been reported to be effective against various viruses [110, 111], but there are few reports on its effectiveness against influenza viruses. Hanada et al. [63] previously reported the antiviral effects of 8-PN in plants; 8-PN showed stronger activity than naringenin. In addition, I reported that the antiviral effect depends on the structure of the flavonoids [103]. Here, I investigated the anti-influenza effects of naringenin derivatives and their kinetics in cells.

First, I focused on the relationship between the structure and activity of naringenin and its derivatives, including prenylated naringenin. I hypothesized that the structure of the substituents was a factor in viral activity and synthesized 13 compounds with substituents with different properties. Naringenin showed antiviral activity, while naringenin- 4',7'-diacetate lost its activity. I predicted that the diacetyl structure is involved in the expression of activity. However, compound **1c** exhibited antiviral activity at 42 μM. These results suggest that the 8-position substituent, rather than the 4'and 7' positions, is essential for anti-influenza virus activity. Additionally, the activity was expressed by the iso-pentyl group (**1c** and **1d**); however, **1b** and **1e** were not active. These results suggested that the dimethyl structure of the carbon chain is involved in the expression of activity. The epoxide group (**1a**) had decreased anti-influenza virus activity. Therefore, substituents (hydrocarbon chains) that do not exhibit coordinating properties in the flavanone skeleton are desirable.

Next, the antiviral activities of the 6-position derivatives were evaluated. Since the activity of 6-allylnaringenin (**2a**) decreased, highlighting the effect of the length of the

carbon chain rather than the electronic effect of the substituents, it was inferred that a steric factor was also involved in the 6-position derivatives. The effect of the double-bond site in the substituent is thought to be due to the coordinating property or partial planarity, but no clear factor could be confirmed. However, unsaturated substituents would be desirable, as compounds with double bonds show stronger activity (Table 3-1, -2, -3). In addition, the **2c** and **2d** results suggest that cyclohexane may be a steric obstacle for activity, and the steric size suitable for the anti-influenza virus effect was the dimethyl structure in the prenyl group, which has a branched structure. Therefore, 8-PN and 6-PN showed the strongest activities among the synthesized derivatives group, and the prenyl group dramatically affected the anti-influenza virus effect. The results of the 8- and 6-position derivatives suggest that the steric factors of the compounds are deeply involved in anti-influenza virus activity.

In addition, based on the research report by Murota et al. [112], I speculated that the prenyl group has the potential to enhance affinity with cell lipid membranes and increase cellular uptake. To confirm this hypothesis, I exposed cultured cells to naringenin and prenylated naringenin and observed them using fluorescence microscopy. Cellular uptake experiments confirmed the characteristic fluorescence intensity depending on the structure of the compound (Figure 3-1.–3-3). After 180 min of exposure, many compounds showed a plateau in MDCK cells, and **1d**, 8-PN, and 6-PN showed high fluorescence intensities in each derivative group. These results indicate that the prenyl and isopentyl groups at the 8-position enhance the affinity to cells and to the cell membrane or other uptake factors. When further cellular distribution was examined by fluorescence microscopy and compared to naringenin, the distribution of fluorescence was clearly confirmed (Figure 3-4). Tanaka et al. [113] reported that the cellular uptake

of 8-PN in HEK293 cells was higher than that of naringenin, and similar results were obtained in MDCK cells. While 8-PN was localized throughout the nucleus and cytoplasm, 6-PN was localized in the periphery of the cytoplasm. This kinetics can be attributed to the *in vivo* interactions of each compound. Low molecular weight compounds such as flavonoids are known to bind to proteins *in vivo*, and albumin is also used as an indicator of *in vivo* nutrition [114]. Flavonoids have also been reported to have a high affinity for intracellular proteins [115, 116], which is not only due to the affinity of the compound to the cell membrane, but also due to the interaction with intracellular proteins. The fact that the medium contained approximately 20 nM albumin during fluorescence microscopy and about 60 μM at the time-of-addition assay may also affect the results. To confirm the kinetics of prenylated naringenin, I prepared cells saturated with the compound. After saturation, the cells were exposed to DMEM containing 1% FBS and fluorescence was observed at each time point. Consequently, the intracellular amount of 8-PN decreased slowly, and that of 6-PN decreased dramatically (Figure 3-5 and 3-6). These results indicate that the intracellular residence time of prenylated flavonoids increased and affected the efflux time. Mukai et al. [117] reported the intracellular localization of flavonols and flavones in fluorescence microscopy experiments; their behaviors differed depending on the substituent. To clarify the anti-influenza virus mechanism of each flavonoid, it is necessary to investigate the intracellular uptake mechanisms, such as endocytosis, passive diffusion, and membrane transporters, in detail. The kinetics of this prenylated compound are of great interest and provide pharmacological insights into antiviral strategies.

This result suggests different intracellular kinetics, which may also be involved in the antiviral effects. Although 8-PN and 6-PN commonly block the late stage of viral growth

(6–8 h), a time-of-addition assay revealed that the inhibitory effect on the antiviral effect differs depending on the position of the substituent (Figure 3-7-A). Interestingly, 6-PN showed a different inhibitory effect than 8-PN (after infection to 4–6 h). In the influenza A virus, it has been reported that assembly of viral proteins and budding of mature virus particles take place in cells approximately 6–8 h after infection [47]. This suggests the possibility of inhibiting the growth process until viral maturation. DMEM containing BSA was used for the time-of-addition assay, from the results shown in Figures 3-5 and 3-6, it is likely that part of the prenylated naringenin in the cells was bound to albumin in the medium. This binding may be involved in the intracellular and extracellular kinetics. Interactions between *in vivo* substances and flavonoids may affect the kinetics and anti-influenza virus efficacy. This experiment, in addition to Hanada's report [63], indicates that prenylation of naringenin confers broad antiviral effects on influenza A and B viruses, broadening its potential as a novel antiviral agent. Moreover, in the process of chemical synthesis, diastereomeric mixtures of naringenin derivatives were generated and their separation was difficult due to their physical properties. Future research will focus on the effects of structure mixtures and subtle structural differences. However, this work is one of the few reports investigating the biological properties of flavonoid structures against influenza virus.

It was able to elucidate some of the structure-activity relationships of flavanone derivatives against influenza viruses, providing important information for antiviral strategies. Further study of this property may result in qualitative improvements in the pharmacological activity of drugs against influenza viruses.

Conclusion

It is revealed that anti-influenza virus activity of WWMJ *in vitro* and *in vivo*. Also, WWMJ inhibited the H1N1, H3N2 and B types of influenza virus strains including oseltamivir-resistant strain. The action of mechanism of WWMJ was inhibited virus growth steps, such as virus adsorption to the host cells and virus replication (especially, after infection to 4-8h, 4-6h). One of the causes of WWMJ activity is polyphenols, and many natural compounds were detected.

The results of flavonoid activity will contribute to current efforts in the design and development of the next generation of anti-influenza drugs by identifying the structure of flavonoids, particularly the binding sites of hydroxyl groups, on their anti-influenza viral effects. So, an understanding of the interactions of natural compounds and other factors in infected cells is important to obtain new insights for the treatment of viral infections.

Naringenin, a flavanone found mainly in vegetables and fruits, has been reported to possess various physiological functions, including antiviral activity. I investigated the relationship between the antiviral activity of naringenin, prenylated naringenin, and their derivatives against influenza infection as well as the cellular uptake of these flavanones. In the structure of naringenin, the substituent that enhances antiviral activity is the prenyl group, and its structure and position have a significant effect on its cell permeability.

This doctoral thesis also present perspectives on the therapeutic applications of flavonoids against viral infections in the future.

Acknowledgments

References

1. Sampath S, Khedr A, Qamar S *et al*. Pandemics throughout the history. *Cureus*, **2021**, 13, e18136.   https://doi.org/10.7759/cureus.18136.

2. ICTV -9th Reports. **2011**, https://ictv.global/report_9th.

3. Odagiri T, Ishida H, Li JY *et al*. Antigenic heterogeneity among phylogenetic clusters of influenza D viruses. *J Vet Med Sci*, **2018**, 80,1241–1244. https://doi.org/10.1292/jvms.18-0157.

4. CDC-Influenza (About Flu). **2022**, https://www.cdc.gov/flu/about/viruses/types.htm

5. Kondrich J, Rosenthal M. Influenza in children. *Curr Opin Pediatr,* **2017**, 29, 297-302. https://doi.org/10.1097/MOP.0000000000000495.

6. Mauskopf J, Klesse M, Lee S *et al*. The burden of influenza complications in different high-risk groups: a targeted literature review. *J Med Econ*, **2013**, 16, 264-277. https://doi.org/10.3111/13696998.2012.752376.

7. Coleman LA, Waring SC, Irving SA *et al*. Evaluation of obesity as an independent risk factor for medically attended laboratory-confirmed influenza. *Influenza Other Respir Viruses*, **2013**, 7, 160-167. https://doi.org/10.1111/j.1750-2659.2012.00377.x.

8. Luo M. Influenza virus entry. *Adv Exp Med Biol*, **2012**, 726, 201-221. https://doi.org/10.1007/978-1-4614-0980-9_9.

9. Yewdell JW. Antigenic drift: Understanding COVID-19. *Immunity*, **2021**, 54, 2681-2687. https://doi.org/10.1016/j.immuni.2021.11.016.

10. Zhang J, Ye H, Li H *et al*. Evolution and antigenic drift of influenza A (H7N9) viruses, china, 2017-2019. *Emerg Infect Dis*, **2020**, 26, 1906-1911. https://doi.org/10.3201/eid2608.200244.

11. Choo D, Hossain M, Liew P *et al*. Side effects of oseltamivir in end-stage renal failure patients. *Nephrol Dial Transplant*, **2011**, 26, 2339-2344. https://doi.org/10.1093/ndt/gfq737.

12. Mohan T, Nguyen HT, Kniss K *et al*. Cluster of oseltamivir-resistant and hemagglutinin antigenically drifted influenza A(H1N1) pdm09 viruses, texas, USA, January 2020. *Emerg Infect Dis,* **2021**, 27, 1953-1957. https://doi.org/10.3201/eid2707.204593.

13. Patel MC, Mishin VP, De La Cruz JA *et al*. Detection of baloxavir resistant influenza A viruses using next generation sequencing and pyrosequencing methods. *Antiviral Res*, **2020**, 182, 104906. https://doi.org/10.1016/j.antiviral.2020.104906.

14. Goldhill DH, Yan A, Frise R *et al*. Favipiravir-resistant influenza A virus shows potential for transmission. *PLoS Pathog*, **2021**, 17, e1008937. https://doi.org/10.1371/journal.ppat.1008937.

15. Bai GR, Chittaganpitch M, Kanai Y *et al*. Amantadine- and oseltamivir-resistant variants of influenza A viruses in Thailand. *Biochem Biophys Res Commun*, **2009**, 390, 897-901. https://doi.org/10.1016/j.bbrc.2009.10.071.

16. Choi WY, Kim S, Lee N *et al*. Amantadine-resistant influenza A viruses isolated in South Korea from 2003 to 2009. *Antiviral Res*, **2009**, 84,199-202. https://doi.org/10.1016/j.antiviral.2009.08.006.

17. Akbik D, Ghadiri M, Chrzanowski W *et al*. Curcumin as a wound healing agent.

Life Sci, **2014**, 116,1-7. https://doi.org/10.1016/j.lfs.2014.08.016.

18. Wen K, Fang X, Yang J *et al*. Recent research on flavonoids and their biomedical applications. *Curr Med Chem,* **2021**, 28, 1042-1066. https://doi.org/10.2174/0929867327666200713184138.

19. Elkashty OA, Tran SD. Sulforaphane as a promising natural molecule for cancer prevention and treatment. *Curr Med Chem,* **2021**, 41, 250-269. https://doi.org/10.1007/s11596-021-2341-2.

20. Badshah SL, Faisal S, Muhammad A *et al*. Antiviral activities of flavonoids. *Biomed Pharmacother,* **2021**, 140, 111596. https://doi.org/10.1016/j.biopha.2021.111596

21. Kamei M, Nishimura H, Takahashi T *et al*. Anti-influenza virus effects of cocoa. *J Sci Food Agric,* **2016**, 96, 1150-1158. https://doi.org/10.1002/jsfa.7197.

22. Lee JB, Miyake S, Umetsu R *et al*. Anti-influenza A virus effects of fructan from Welsh onion (*Allium fistulosum L.*). *Food Chem,* **2012**, 134, 2164-2168. https://doi.org/10.1016/j.foodchem.2012.04.016.

23. Sekizawa H, Ikuta K, Mizuta K *et al*. Relationship between polyphenol content and anti-influenza viral effects of berries. *J Sci Food Agric,* **2013**, 93, 2239-2241. https://doi.org/10.1002/jsfa.6031.

24. Makau JN, Watanabe K, Mohammed MMD *et al*. Antiviral activity of peanut (*Arachis hypogaea* L.) skin extract against human influenza viruses. *J Med Food*, **2018**, 21, 774-777. https://doi.org/ 10.1089/jmf.2017.4121.

25. Peck H, Moselen J, Brown SK *et al*. Report on influenza viruses received and tested by the melbourne WHO collaborating centre for reference and research on influenza in 2019. *Commun Dis Intell (2018)*, **2021**, 16, 45. https://doi.org/10.33321/cdi.2021.45.43.

26. O'Neill G, Aziz A, Kuba M *et al*. Report on influenza viruses received and tested by the melbourne WHO collaborating centre for reference and research on influenza during 2020-2021. *Commun Dis Intell (2018)*, **2022**, 26, 46. https://doi.org/10.33321/cdi.2022.46.63.

27. Centers for Disease Control and Prevention (CDC). Swine influenza A (H1N1) infection in two children—Southern California, March-April 2009. *MMWR Morb Mortal Wkly Rep*, **2009**, 58, 400-402.

28. Dortmans JC, Dekkers J, Wickramasinghe IN *et al*. Adaptation of novel H7N9 influenza A virus to human receptors. *Sci Rep*, **2013**, 3:3058. https://doi.org/10.1038/srep03058.

29. Ducatez MF, Pelletier C, Meyer G. Influenza D virus in cattle, France, 2011-2014. *Emerg Infect Dis*, **2015**, 21, 368-371. https://doi.org/10.3201/eid2102.141449.

30. Song H, Qi J, Khedri Z *et al*. An open receptor-binding cavity of hemagglutinin-esterase-fusion glycoprotein from newly-identified Influenza D virus: basis for its broad cell tropism. *PLoS Pathog*, **2016**, 12: e1005411.https://doi.org/10.1371/journal.ppat.1005411.

31. Danciu C, Avram S, Pavel IZ *et al*. Main isoflavones found in dietary sources as natural anti-inflammatory agents. *Curr Drug Targets*, **2018**, 19, 841-853. https://doi.org/10.2174/1389450118666171109150731.

32. Kim M, Im S, Cho YK *et al*. Anti-obesity effects of soybean embryo extract and enzymatically-modified isoquercitrin. *Biomolecules*, **2020**, 10, 1394. https://doi.org/10.3390/biom10101394.

33. Cao L, Lee SG, Lim KT *et al*. Potential anti-aging substances derived from

seaweeds. *Mar Drugs,* **2020**, 18, 564. https://doi.org/10.3390/md18110564.

34. Park S, Kim JI, Lee I *et al*. Aronia melanocarpa and its components demonstrate antiviral activity against influenza viruses. *Biochem Biophys Res Commun*, **2013**, 440,14-19. https://doi.org/10.1016/j.bbrc.2013.08.090.

35. Nagai E, Iwai M, Koketsu R *et al*. Inhibition of influenza virus replication by adlay tea. *J Sci Food Agric*, **2018**, 98,1899-1905. https://doi.org/10.1002/jsfa.8671.

36. Nagai E, Iwai M, Koketsu R *et al*. Anti-influenza virus activity of adlay tea components. *Plant Foods Hum Nutr*, **2019**, 74, 538-543. https://doi.org/ 10.1007/s11130-019-00773-3.

37. Kanazawa R, Morimoto R, Horio Y *et al*. Inhibition of influenza virus replication by Apiaceae plants, with special reference to *Peucedanum japonicum* (Sacna) constituents. *J Ethnopharmacol.* **2022**, 28, 292:115243. https://doi.org/ 10.1016/j.jep.2022.115243.

38. Umar KJ, Hassan LG, Usman H *et al*. Nutritional composition of the seeds of wild melon (*Citrullus ecirrhosus*). *Pak J Biol Sci*, **2013**, 16, 536-540. https://doi.org/ 10.3923/pjbs.2013.536.540.

39. Akashi K, Nishimura N, Ishida Y *et al*. Potent hydroxyl radical-scavenging activity of drought-induced type-2 metallothionein in wild watermelon. *Biochem Biophys Res Commun*, **2004**, 323, 72-78. https://doi.org/ 10.1016/j.bbrc.2004.08.056.

40. Yokota A, Kawasaki S, Iwano M *et al*. Citrulline and DRIP-1 protein (ArgE homologue) in drought tolerance of wild watermelon. *Ann Bot*, **2002**, 89, 825-832. https://doi.org/10.1093/aob/mcf074.

41. Okuno Y, Tanaka K, Baba K *et al*. Rapid focus reduction neutralization test of influenza A and B viruses in microtiter system. *J Clin Microbiol*, **1990**, 28, 1308-

1313. https://doi.org/10.1128/jcm.28.6.1308-1313.1990.

42. Okuno Y, Isegawa Y, Sasao F *et al*. A common neutralizing epitope conserved between the hemagglutinins of influenza A virus H1 and H2 strains. *J Virol*, **1993**, 67, 2552-2558. https://doi.org/10.1128/JVI.67.5.2552-2558.1993.

43. Ueda M, Maeda A, Nakagawa N *et al*. Application of subtype-specific monoclonal antibodies for rapid detection and identification of influenza A and B viruses. *J Clin Microbiol*, **1998**, 36, 340-344. https://doi.org/10.1128/JCM.36.2.340-344.1998.

44. Nakagawa N, Maeda A, Kase T *et al*. Rapid detection and identification of two lineages of influenza B strains with monoclonal antibodies. *J Virol Methods*, *1999*, 79, 113-120. https://doi.org/10.1016/s0166-0934(99)00015-4.

45. Graham RC, karnovsky MJ. The early stages of absorption of injected horseradish peroxidase in the proximal tubules of mouse kidney: ultrastructural cytochemistry by a new technique. *J Histochem Cytochem*, **1966**, 14, 291-302. https://doi.org/10.1177/14.4.291.

46. Dowdle, WR., Kendal, AP, & Noble, GR. Influenza viruses. In E. H. Lennette, & N. J. Schmidt (Eds.), Diagnostic procedures for viral, rickettsial, and chlamydial infections, (5th edn, pp. 585–609). American Public Health Association Publications. **1979**.

47. Furuta Y, Takahashi K, Fukuda Y *et al*. In vitro and in vivo activities of anti-influenza virus compound T-705. *Antimicrob Agents Chemother,* **2002**, 46, 977-981. https://doi.org/10.1128/AAC.46.4.977-981.2002.

48. Mu J, Hirayama M, Sato Y *et al*. A novel high-mannose specific lectin from the green alga Halimeda renschii exhibits a potent anti-influenza virus activity through high-affinity binding to the viral hemagglutinin. *Mar Drugs*, **2017**, 15, 255. https://doi.org/10.3390/md15080255.

49. Barr IG, Hurt AC, Iannello P *et al*. Increased adamantane resistance in influenza A(H3) viruses in Australia and neighbouring countries in 2005. *Antiviral Res*, **2007**, 73, 112-127. https://doi.org/10.1016/j.antiviral.2006.08.002.

50. Seibert CW, Rahmat S, Krammer F *et al*. Efficient transmission of pandemic H1N1 influenza viruses with high-level oseltamivir resistance. *J Virol*, **2012**, 86, 5386-5389. https://doi.org/10.1128/JVI.00151-12.

51. Kim M, Yim JH, Kim SY *et al*. In vitro inhibition of influenza A virus infection by marine microalga-derived sulfated polysaccharide p-KG03. *Antiviral Res*, **2012**, 93, 253-259. https://doi.org/10.1016/j.antiviral.2011.12.006.

52. Haasbach E, Hartmayer C, Hettler A *et al*. Antiviral activity of Ladania067, an extract from wild black currant leaves against influenza A virus in vitro and in vivo. *Front Microbiol*, **2014**, 5, 171. https://doi.org/10.3389/fmicb.2014.00171.

53. Fujiooka Y, Nishide S, Ose T *et al*., A sialylated voltage-dependent Ca^{2+} channel binds hemagglutinin and mediates influenza A virus entry into mammalian cells. *Cell Host Microbe*, **2018**, 23, 809-818.e5. https://doi.org/10.1016/j.chom.2018.04.015.

54. Horio Y, Sogabe R, Shichiri M *et al*. Induction of a 5-lipoxygenase product by daidzein is involved in the regulation of influenza virus replication. *J Clin Biochem Nutr*, **2020**, 66, 36-42. https://doi.org/10.3164/jcbn.19-70.

55. Green RH. Inhibition of multiplication of influenza virus by extracts of tea. *Proc Soc Exp Biol Med,* **1949**, 71, 84. https://doi.org/10.3181/00379727-71-17089p.

56. Song JM, Lee KH, Seong BL. Antiviral effect of catechins in green tea on influenza virus. *Antiviral Res,* **2005**, 68, 66–74. https://doi.org/10.1016/j.antiviral.2005.06.010.

57. Chang CC, You HL, Huang ST. Catechin inhibiting the H1N1 influenza virus associated with the regulation of autophagy. *J Chin Med Assoc*, **2022**, 83, 386–393. https://doi.org/10.1097/JCMA.0000000000000289.

58. Xu J, Xu Z, Zheng W. A review of the antiviral role of green tea catechins. *Molecules*, **2017**, 22, 1337. https://doi.org/10.3390/molecules22081337.

59. Suzuki H, Sasaki R, Ogata Y *et al*. Metabolic profiling of flavonoids in Lotus japonicus using liquid chromatography Fourier transform ion cyclotron resonance mass spectrometry. *Phytochemistry*, **2008**, 69, 99-111. https://doi.org/10.1016/j.phytochem.2007.06.017.

60. Michaelis M, Sithisarn P, Cinatl J Jr. Effects of flavonoid-induced oxidative stress on anti-H5N1 influenza a virus activity exerted by baicalein and biochanin A. *BMC Res Notes*, **2014**, 7, 384. https://doi.org/10.1186/1756-0500-7-384.

61. Di Petrillo A, Orrù G, Fais A *et al*.   Quercetin and its derivates as antiviral potentials: a comprehensive review. *Phytother Res*, **2022**, 36, 266–278. https://doi.org/10.1002/ptr.7309.

62. Zeng W, Jin L, Zhang F *et al*. Naringenin as a potential immunomodulator in therapeutics. *Pharmacol Res*, **2018**, 135, 122–126. https://doi.org/10.1016/j.phrs.2018.08.002.

63. Hanada A, Morimoto R, Horio Y *et al*. Influenza virus entry and replication inhibited by 8-prenylnaringenin from *Citrulls lanatus* var. *Citroides* (Wild watermelon). *Food Sci Nutr,* **2022**, 10, 926–935. https://doi.org/10.1002/fsn3.2725.

64. Wu W, Li R, Li X *et al*. Quercetin as an antiviral agent inhibits influenza A virus (IAV) entry. *Viruses*, **2015**, 8, 6. https://doi.org/10.3390/v8010006.

65. Yan H, Ma L, Wang H *et al*. Luteolin decreases the yield of influenza A virus in vitro by interfering with the coat protein I complex expression. *J Nat Med*, **2019**, 73, 487–496. https://doi.org/10.1007/s11418-019-01287-7.

66. Reiberger R, Radilová K, Kráľ M *et al*. Synthesis and in vitro evaluation of C-7 and C-8 luteolin derivatives as influenza endonuclease inhibitors. *Int J Mol Sci*, **2021**, 22,7735. https://doi.org/10.3390/ijms22147735.

67. Yazawa K, Kurokawa M, Obuchi, M *et al*. Anti-influenza virus activity of tricin, 4',5,7-trihydroxy-3',5'-dimethoxyflavone. *Antivir Chem Chemother*, **2011**, 22, 1-11. https://doi.org/10.3851/IMP1782.

68. Abdal Dayem A, Choi HY, Kim YB *et al*. Antiviral effect of methylated flavonol isorhamnetin against influenza. *PLoS One*, **2015**, 10, e0121610. https://doi.org/10.1371/journal.pone.0121610.

69. Sadati SM, Gheibi N, Ranjbar S *et al*. Docking study of flavonoid derivatives as potent inhibitors of influenza H1N1 virus neuraminidase. *Biomed Rep*, **2019**, 10, 33–38. https://doi.org/10.3892/br.2018.1173.

70. Kitamura K, Erlangga JS, Tsukamoto S *et al*. Daidzein promotes the expression of oxidative physphorylation- and fatty acid oxidation-related genes via an estrogen-related receptor pathway to decrease lipid accumulation in muscle cells. *J Nutr*

Biochem, **2020**, 77, 108315. https://doi.org/10.1016/j.jnutbio.2019.108315.

71. Kanazawa K, Uehara M, Yanagitani H *et al*. Bioavailable flavonoids to suppress the formation of 8-OHdG in HepG2 cells. *Arch Biochem Biophys*, **2006**, 455, 197–203. https://doi.org/10.1016/j.abb.2006.09.003.

72. Kesic MJ, Simmons SO, Bauer R *et al*. Nrf2 expression modifies influenza A entry and replication in nasal epithelial cells. *Free Radic Biol Med*, **2011**, 51, 444–453. https://doi.org/10.1016/j.freeradbiomed.2011.04.027.

73. Chen KK, Minakuchi M, Wuputra K *et al*. Redox control in the pathophysiology of influenza virus infection. *BMC Microbiol*, **2020**, 20, 214. https://doi.org/10.1186/s12866-020-01890-9.

74. Ling JX, Wei F, Li N *et al*. Amelioration of influenza virus-induced reactive oxygen species formation by epigallocatechin gallate derived from green tea. *Acta Pharmacol Sin*, **2012**, 33, 1533–1541. https://doi.org/10.1038/aps.2012.80.

75. Zima V, Radilová K, Kožíšek M *et al*. Unraveling the anti-influenza effect of flavonoids: Experimental validation of luteolin and its congeners as potent influenza endonuclease inhibitors. *Eur J Med Chem*, **2020**, 208, 112754. https://doi.org/10.1016/j.ejmech.2020.112754.

76. Nakashima A, Horio Y, Suzuki K *et al*. Antiviral activity and underlying action mechanism of euglena extract against influenza virus. *Nutrients*, **2021**, 13, 3911. https://doi.org/10.3390/nu13113911.

77. Sawakami T, Karako K., Song P. Behavioral changes adopted to constrain COVID-19 in Japan: What are the implications for seasonal influenza prevention and control? *Glob Health Med*, **2021**, 3, 125-128. https://doi.org/10.35772/ghm.2021.01066.

78. Zhang AJ, Lee AC, Chan JF *et al*. Coinfection by severe acute respiratory syndrome coronavirus 2 and influenza A(H1N1) pdm09 virus enhances the severity of pneumonia in golden. *Clin Infect Dis*, **2021**, 72, e978-e992. https://doi.org/10.1093/cid/ciaa1747.

79. Drake T, Ho A, Turtle L *et al*. Influenza infection in patients hospitalized with COVID-19: *Rapid Report from CO-CIN Data*; Proceedings of the 59 SAGE Meeting; London, UK. 24 September **2020**.

80. Honigsbaum M. Revisiting the 1957 and 1968 influenza pandemics. *Lancet*, **2020**, 395, 1824-1826. https://doi.org/10.1016/S01406736(20)31201-0.

81. Elderfield R, Barclay W. Influenza pandemics. *Adv Exp Med Biol*, **2011**, 719, 81-103. https://doi.org/10.1007/978-1-4614-0204-6_8.

82. Boonnak K, Mansanguan C, Schuerch D *et al*. Molecular characterization of seasonal influenza A and B from hospitalized patients in thailand in 2018-2019. *Viruses*, **2021**, 13, 977. https://doi.org/10.3390/v13060977.

83. Kim HM, Lee N, Kim M *et al*. Characterization of neuraminidase inhibitor-resistant influenza virus isolates from immunocompromised patients in the republic of korea. *Virol J*, **2020**, 17, 94. https://doi.org/10.1186/s12985-020-01375-1.

84. Hayden FG, Sugaya N, Hirotsu N *et al*. Baloxavir Marboxil for uncomplicated influenza in adults and adolescents. *N Engl J Med*, **2018**, 379, 913-923. https://doi.org/10.1056/NEJMoa1716197.

85. Lampejo T. Influenza and antiviral resistance: an overview. *Eur J Clin Microbiol Infect Dis*, **2020**, 39, 1201-1208. https://doi.org/10.1007/s10096-020-03840-9.

86. Miles EA, Calder PC. Effects of citrus fruit juices and their bioactive components on inflammation and immunity: a narrative review. *Front Immunol*, **2021**, 12, 712608. https://doi.org/10.3389/fimmu.2021.712608.

87. Ali MY, Sina AA, Khandker SS *et al*. Nutritional composition and bioactive compounds in tomatoes and their impact on human health and disease: a review. *Foods*, **2020**, 10, 45. https://doi.org/10.3390/foods10010045.

88. Santhi VP, Masilamani P, Sriramavaratharajan V *et al*. Therapeutic potential of phytoconstituents of edible fruits in combating emerging viral infections. *J Food Biochem*, **2021**, 45, e13851. https://doi.org/10.1111/jfbc.13851.

89. Hernández-Aquino E, Muriel P. Beneficial effects of naringenin in liver diseases: molecular mechanisms. *World J Gastroenterol*, **2018**, 24, 1679-1707. https://doi.org/10.3748/wjg.v24.i16.1679.

90. Chen Z, Chen P, Wu H *et al*. Evaluation of naringenin as a promising treatment option for COPD based on literature review and network pharmacology. *Biomolecules*, **2020**,10,1644. https://doi.org/ 10.3390/biom10121644.

91. Khan A, Ikram M, Hahm JR *et al*. Antioxidant and anti-inflammatory effects of citrus flavonoid hesperetin: special focus on neurological disorders. *Antioxidants (Basel)*, **2020**, 9, 609. https://doi.org/10.3390/antiox9070609.

92. Motallebi M, Bhia M, Rajani HF *et al*. Naringenin: a potential flavonoid phytochemical for cancer therapy. *Life Sci*, **2022**, 305, 120752. https://doi.org/10.1016/j.lfs.2022.120752.

93. Thayumanavan G, Jeyabalan S, Fuloria S *et al*. Silibinin and naringenin against bisphenol A-Induced neurotoxicity in zebrafish model-potential flavonoid molecules for new drug design, development, and therapy for neurological disorders. *Molecules*, **2022**, 27, 2572. https://doi.org/10.3390/molecules27082572.

94. Salehi B, Fokou PVT, Sharifi-Rad M *et al*. The therapeutic potential of naringenin: a review of clinical trials. *Pharmaceuticals (Basel)*, **2019**, 12, 11. https://doi.org/10.3390/ph12010011.

95. Montenegro-Landívar MF, Tapia-Quirós P, Vecino X *et al*. Polyphenols and their potential role to fight viral diseases: An overview. *Sci Total Environ*, **2021**, 801, 149719. https://doi.org/10.1016/j.scitotenv.2021.149719.

96. Venturelli S, Niessner H, Sinnberg T *et al*. 6- and 8-prenylnaringenin, novel natural histone deacetylase inhibitors found in hops, exert antitumor activity on melanoma cells. *Cell Physiol Biochem,* **2018**, 51, 543-556. https://doi.org/10.1159/000495275.

97. Liu M, Hansen PE, Wang G *et al*. Pharmacological profile of xanthohumol, a prenylated flavonoid from hops (*Humulus lupulus*). *Molecules*, **2015**, 20, 754-779. https://doi.org/10.3390/molecules20010754.

98. Štulíková K, Karabín M, Nešpor J *et al*. Therapeutic perspectives of 8-prenylnaringenin, a potent phytoestrogen from hops. *Molecules*, **2018**, 23, 660. https://doi.org/10.3390/molecules23030660.

99. Mukai R. Prenylation enhances the biological activity of dietary flavonoids by altering their bioavailability. *Biosci Biotechnol Biochem*, **2018**, 82, 207–215. https://doi.org/10.1080/09168451.2017.1415750.

100. Grienke U, Richter M, Walther E *et al*. Discovery of prenylated flavonoids with dual activity against influenza virus and Streptococcus pneumoniae. *Sci Rep*, **2016**, 6, 27156. https://doi.org/10.1038/srep27156.

101. Seliger JM, Misuri L, Maser E *et al*. The hop-derived compounds xanthohumol, isoxanthohumol and 8-prenylnaringenin are tight-binding inhibitors of human aldo-keto reductases 1B1 and 1B10. *J Enzyme Inhib Med Chem*, **2018**, 33, 607-614. https://doi.org/10.1080/14756366.2018.1437728.

102. Tronina T, Popłoński J, Bartmańska A. Flavonoids as phytoestrogenic components of hops and beer. *Molecules*, **2020**, 25, 4201. https://doi.org/10.3390/molecules25184201.

103. Morimoto R, Hanada A, Matsubara C *et al*. Anti-influenza A virus activity of flavonoids *in vitro*: a structure-activity relationship. *J Nat Med*, **2022**, 77, 219-227. https://doi.org/10.1007/s11418-022-01660-z.

104. Mukai R, Fujikura Y, Murota K *et al*. Prenylation enhances quercetin uptake and reduces efflux in Caco-2 cells and enhances tissue accumulation in mice fed long term. *J Nutr*, **2013**, 143, 1558–1564. https://doi.org/10.3945/jn.113.176818.

105. Morimoto R, Yoshioka K, Nakayama M *et al*. Juice of *citrullus lanatus* var. *citroides* (wild watermelon) inhibits the entry and propagation of influenza viruses *in vitro* and *in vivo*. *Food Sci Nutr*, **2021**, 9, 544–552. https://doi.org/10.1002/fsn3.2023.

106. Wolff H, Motyl M, Hellerbrand C *et al*. Xanthohumol uptake and intracellular kinetics in hepatocytes, hepatic stellate cells, and intestinal cells. *J Agric Food Chem*, **2011**, 59, 12893-12901. https://doi.org/10.1021/jf203689z.

107. Liu CH, Jassey A, Hsu HY *et al*. Antiviral activities of silymarin and derivatives. *Molecules*, **2019**, 24, 1552. https://doi.org/10.3390/molecules24081552.

108. Di Petrillo A, Orrù G, Fais A *et al*. Quercetin and its derivates as antiviral potentials: A comprehensive review. *Phytother Res*, **2022**, 36, 266-278. https://doi.org/10.1002/ptr.7309.

109. Tian Y, Sang H, Liu M *et al*. Dihydromyricetin is a new inhibitor of influenza polymerase PB2 subunit and influenza-induced inflammation. *Microbes Infect*, **2020**, 22, 254-262. https://doi.org/10.1016/j.micinf.2020.05.021.

110. Frabasile S, Koishi AC, Kuczera D *et al*. The citrus flavanone naringenin impairs dengue virus replication in human cells. *Sci Rep*, **2017**, 7, 41864. https://doi.org/10.1038/srep41864.

111. Tutunchi H, Naeini F, Ostadrahimi A *et al*. Naringenin, a flavanone with antiviral and anti-inflammatory effects: a promising treatment strategy against COVID-19. *Phytother Res*, **2020**, 34, 3138-3147. https://doi.org/10.1002/ptr.6781.

112. Murota K, Shimizu S, Miyamoto S *et al*. Unique uptake and transport of isoflavone aglycones by human intestinal CACO-2 cells: comparison of isoflavonoids and flavonoids. *J Nutr*, **2002**, 132, 1956-1961. https://doi.org/10.1093/jn/132.7.1956.

113. Tanaka Y, Okuyama H, Nishikawa M *et al*. 8-Prenylnaringenin tissue distribution and pharmacokinetics in mice and its binding to human serum albumin and cellular uptake in human embryonic kidney cells. *Food Sci Nutr*, **2022**, 10, 1070-1080. https://doi.org/10.1002/fsn3.2733.

114. De Simone G, di Masi A, Ascenzi P. Serum albumin: a multifaced enzyme. *Int J Mol Sci*, **2021**, 22, 10086. https://doi.org/10.3390/ijms221810086.

115. Bolli A, Marino M, Rimbach G *et al*. Flavonoid binding to human serum albumin. *Biochem Biophys Res Commun*, **2010**, 398, 444-449. https://doi.org/10.1016/j.bbrc.2010.06.096.

116. Joyner PM. Protein adducts and protein oxidation as molecular mechanisms of flavonoid bioactivity. *Molecules*, **2021**, 26, 5102. https://doi.org/10.3390/molecules26165102.

117. Mukai R, Shirai Y, Saito N *et al*. Subcellular localization of flavonol aglycone in hepatocytes visualized by confocal laser scanning fluorescence microscope. *Cytotechnology*, **2009**, 59, 177-182. https://doi.org/10.1007/s10616-009-9206-z.